RECHARGE AND GROUNDWATER CONDITIONS IN THE WESTERN REGION OF THE ROSWELL BASIN

by

Christopher J. Duffy
Graduate Research Assistant
New Mexico Institute of Mining and Technology

Lynn W. Gelhar
Professor of Hydrology
New Mexico Institute of Mining and Technology

Gerardo Wolfgang Gross
Professor of Geophysics
New Mexico Institute of Mining and Technology

PARTIAL TECHNICAL COMPLETION REPORT

Project No. A-055-NMEX

August 1978

New Mexico Water Resources Research Institute
in cooperation with
Department of Geoscience
New Mexico Institute of Mining and Technology

The work upon which this publication is based was supported in part by funds provided through the New Mexico Water Resources Research Institute by the United States Department of the Interior, Office of Water Resources Research and Technology, as authorized under the Water Resources Research Act of 1964, Public Law 88-379, under project number A-055-NMEX and by the State of New Mexico through state appropriations.

The purpose of WRRI technical reports is to provide a timely outlet for research results obtained on projects supported in whole or in part by the Institute. Through these reports we are promoting the free exchange of information and ideas and hope to stimulate thoughtful discussion and action which may lead to resolution of water problems. The WRRI, through peer review of draft reports, attempts to substantiate the accuracy of information contained in its reports but the views expressed are those of the author(s) and do not necessarily reflect those of the WRRI or its reviewers.

ABSTRACT

An examination of recharge and groundwater conditions of the western region of the Roswell basin is presented. Recharge mechanisms are proposed on the basis of several long record observation wells. Water levels with long trends are associated with recharge from areal precipitation. It is thought that several years of above average rainfall are necessary to increase groundwater storage significantly. A fluctuating cyclic response is associated with channel leakage from streams in the study area. This recharge mechanism was verified using a stochastic stream-aquifer model applied to the Rio Hondo and Rio Peñasco drainages. With this model, channel leakage and aquifer parameters could be estimated.

The two types of water level response are associated with characteristic tritium levels. High tritium levels in wells near streams verify a fast recharge component indicated by the model. For wells not located near streams in the intake area and for wells in the Principal Aquifer, low tritium values are found. These wells indicate longer residence times than previously suggested. It seems likely that precipitation on the region outside the Principal Intake Area supplies a significant portion of total recharge to the Principal Aquifer.

TABLE OF CONTENTS

LIST OF FIGURES

LIST OF TABLES

Table Page

LIST OF SYMBOLS

Symbol	Definition	Dimension
β_0, β_1	Coefficients of linear regression.	
$\delta(x)$	Dirac delta function for x.	(1/L)
$E(x,y.t)$	Recharge rate to the water table.	(L/T)
$\Theta(f,x)$	Phase angle between two series.	(Radians)
ν	Degrees of freedom.	
ρ	Correlation coefficient.	
τ	Lag number.	
$\phi_{hh}(\omega,x)$	Spectrum of hydraulic head.	$(L)^2$
$\phi_{qh}(\omega,x)$	Cross-spectrum of hydraulic head and recharge (channel leakage).	(L^3/T)
$\phi_{qq}(\omega)$	Spectrum of recharge rate.	(L^4/T^2)
$\phi_{Q\hat{h}}(\omega,x)$	Cross-spectrum of hydraulic head and streamflow.	(L^4/T)
$\phi_{QQ}(\omega)$	Spectrum of stream discharge.	(L^6/T^2)
$\hat{\phi}$	Estimator.	
ω	Angular frequency.	$\left(\frac{\text{Radians}}{T}\right)$
a	Streambed leakage parameter or fraction of streamflow which is lost to the groundwater.	(1/L)
$dZ_h(\omega,x)$	Complex Fourier amplitude of hydraulic head fluctuations.	(L)
$dZ_Q(\omega)$	Complex Fourier amplitude of stream discharge fluctuations.	(L^3/T)
f	Ordinary frequency.	$\left(\frac{\text{cycles}}{T}\right)$
$h(x,y,t)$	Hydraulic head.	(L)

Symbol	Definition	Dimension
$\bar{h}$	Mean hydraulic head.	(L)
h'	Fluctuations in hydraulic head about the mean.	(L)
i	$\sqrt{-1}$	
$q(x,t)$	Volumetric recharge rate per foot of channel.	(L^2/T)
$\bar{q}$	Mean recharge rate.	(L^2/T)
q'	Fluctuations in recharge rate about the mean value.	(L^2/T)
s	Estimated standard deviation.	
A_{Qh}	Amplitude of spectrum.	
K_x, K_y	Hydraulic conductivity in the x and y directions.	(L/T)
Ln (or ℓn)	Natural logarithm.	
M	Maximum number of lags.	
N	Total length of record or sample size.	
$p(x)$	Probability density function.	
$p(x_1,x_2)$	Joint probability density function.	
$Q(t)$	Stream discharge.	(L^3/T)
$Q'(t)$	Fluctuations in stream discharge about the mean.	(L^3/T)
$R_{hh}(\tau)$	Autocovariance of hydraulic head.	(L^2)
$R_{qq}(\tau)$	Autocovariance of recharge rate.	(L^4/T^2)
$R_{qh}(\tau)$	Cross-covariance of head and recharge.	(L^3/T)
$R_{Qh}(\tau)$	Cross-covariance of head and discharge.	(L^4/T)

Symbol	Definition	Dimension
$R_{QQ}(\tau)$	Autocovariance of stream discharge.	(L^6/T^2)
$\hat{R}$	Estimator.	
S	Storage coefficient or effective porosity.	
T	Transmissivity.	(L^2/T)
x	Distance from stream to well.	(L)

ACKNOWLEDGMENTS

The writers are indebted to many persons whose assistance and advice were essential to this report.

Mr. Ray Wyche, manager of the Pecos Valley Artesian Conservancy District, made available water level records for a number of observation wells in the study region, and he also contributed his time and experience generously. Mr. Ed Welder of the U. S. Geological Survey in Albuquerque was instrumental to the authors' recognition of the problem. Development of the spectral theory and interpretation of results was accomplished with the help of Dr. Allan Gutjahr of the Department of Mathematics at New Mexico Tech.

The authors wish to thank the New Mexico State Engineer Office in Roswell for making available geologic and hydrologic information essential to the report.

The advice of Mr. Kay Havenor, CPG, of Roswell on the hydrogeology of the study region is gratefully acknowledged.

The writers wish to thank the numerous individuals who helped collect water level data, water samples for tritium determinations, and geologic information, especially: Rich Naff, Adel Bakr, Paul Davis, Ralph Wilcox, Roberta Hoy and Sabine Lutkemeier.

The generous cooperation of ranchers and farmers of the Roswell basin was essential to the completion of this report.

INTRODUCTION

This report attempts to quantify the groundwater resources of the Yeso and Glorieta aquifers in the western Roswell basin. The importance of these aquifers to the overall water resources of the basin has been suggested by several authors. M. S. Hantush (1957, p. 8) states, "the greater precipitation on the area outside the 'principal intake area', and the principal movement of both perched and deep water,....., suggest that significant amounts of water ultimately will enter the San Andres Formation and thus contribute to the recharge of the basin". The Principal Intake Area, as defined by Fiedler and Nye (1933), is located just west of the confined beds of the Principal Aquifer, where the water table is in the San Andres Formation. As reported by Gross et al. (1976), several years of basin-wide tritium sampling generally indicate low tritium values for groundwater in both the intake area and the Principal Aquifer; this suggests significant recharge from the less permeable western region.

In this report, recharge mechanisms in the study area are proposed on the basis of water level response and tritium sampling over several years. The stream-aquifer recharge process is examined in detail using an inverse method with stochastic variables in the model. The importance of the western region of the Roswell basin in terms of its underflow or leakage to the Principal Intake Area is examined, and an estimate of annual underflow is computed to demonstrate its importance.

Section 1

SUMMARY OF HYDROGEOLOGY AND PREVIOUS WORK

General

The area of investigation for this report is the western region of the Roswell basin (Fig. 1). The geographic setting of the basin is southeastern New Mexico, bordering the Pecos River, the principal drainage. The Capitan, Sacramento and Guadalupe Mountains form the western physiographic boundary, and the east slope of the Pecos River is the accepted boundary in the east (Fig. 2). The Arroyo del Macho and the Seven Rivers hills are the northern and southern limits respectively. The western mountains are drained by several tributaries of the Pecos. From north to south they are: Arroyo del Macho, Salt Creek, Rio Hondo, Rio Felix, Rio Peñasco and Seven Rivers. Of particular importance to this investigation are the Rio Hondo and Rio Peñasco.

The eastern groundwater boundary of this investigation occurs where the regional water table intersects the contact between the Glorieta Sandstone and the San Andres Formation. A rapid decrease in the hydraulic gradient is observed as groundwater discharges from the less permeable Glorieta Sandstone in the west to the highly permeable San Andres Formation. The northern, southern and western groundwater boundaries of the study area are assumed to coincide with the physiographic boundaries of the basin.

The climate of the Roswell basin is generally semi-arid. Rainfall distribution over the basin is influenced by altitude, with

NEW MEXICO BUREAU OF MINES AND MINERAL RESOURCES

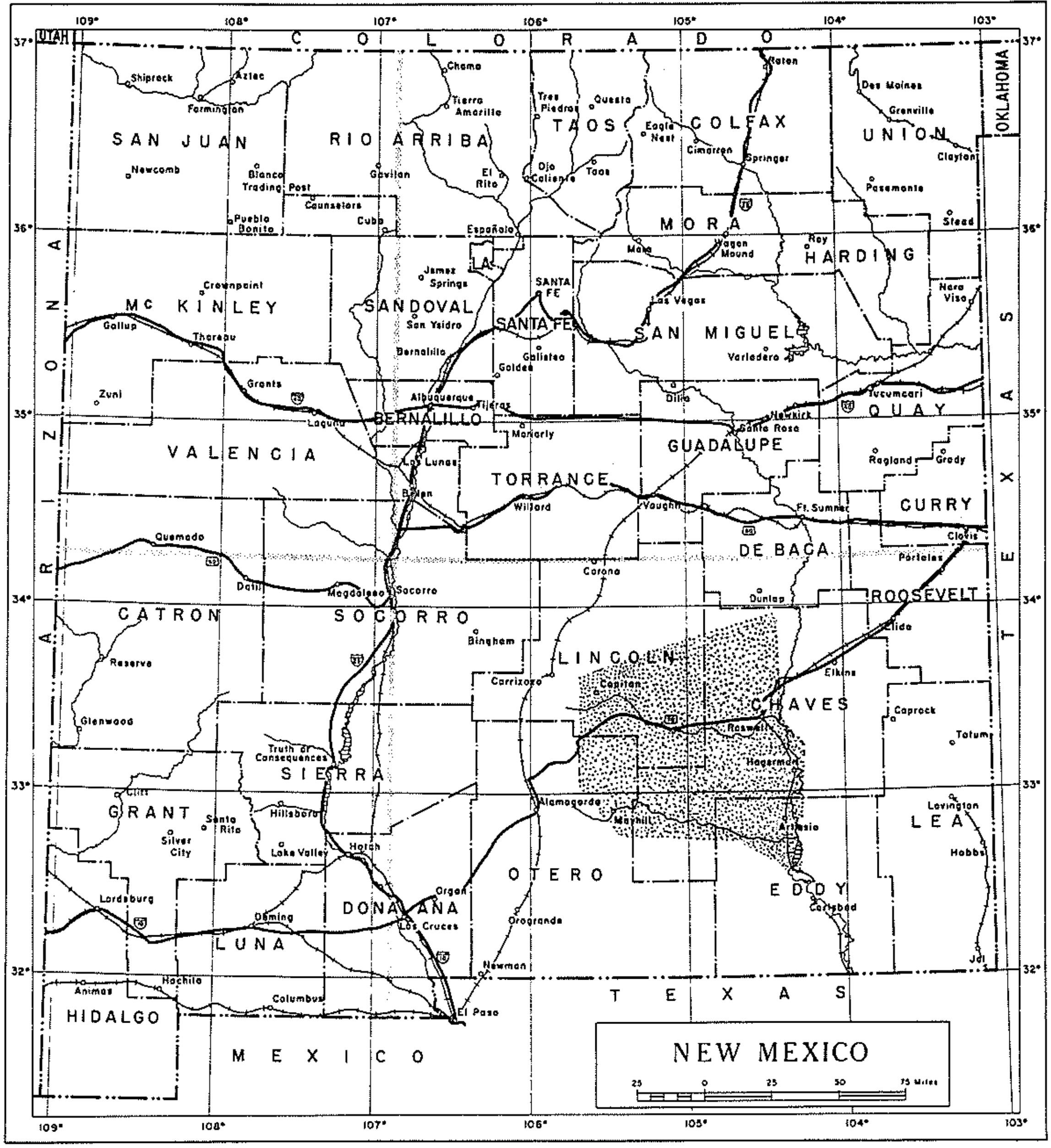

Fig. 1: Location of the groundwater basin.

the eastern plains receiving 8 to 12 inches of rain annually, and the upland areas more than 20 inches. The majority of rainfall occurs during the summer thundershower season, June-September. High temperatures and low humidity combine to produce high rates of evaporation on surface water and irrigated land. The demand for water from municipal, farming and ranching interests has led to large-scale development of groundwater and surface water supplies. The significance of the western region to the overall water resources of the Roswell basin is emphasized in this report.

Previous Investigations

A good deal of work has been devoted to understanding the hydrogeology of the Roswell basin; only a brief summary of previous research is presented here.

One of the earliest comprehensive studies on the entire basin was made by Fiedler and Nye (1933). This paper describes in considerable detail the geology and hydrology of the region. Renicke (1926) gave a brief description of the geology of the western Rio Peñasco drainage. Bean (1949) reported on the geology and hydrogeology of the Hondo Reservoir; and Theis (1951) outlined the effects of floodwater storage in the Hondo Reservoir and its relation to the Principal Aquifer.

In 1957 a quantitative hydrologic investigation of the Roswell basin was reported by M. S. Hantush. This study includes estimates of hydraulic conductivity and storativity for the Principal Aquifer and the Principal Intake Area. The latter was proposed by Fiedler and Nye (1933) to be the area adjacent to the Principal Aquifer where most of the recharge was supposed to take place. Motts and Cushman (1964) appraised the artificial recharge capacities of the basin. Mourant's work (1963) details the water resources and geology of the Rio Hondo drainage. Kinney et al. (1968) developed a more detailed picture of the subsurface geology of the basin and its control on groundwater movement. Havenor (1968) investigated the structure, stratigraphy, and hydrogeology of the northern part of the basin.

Rabinowitz and Gross (1972) have proposed a hydrologic model utilizing environmental tritium as a tracer. In a more recent report Gross et al. (1976) suggest that high tritium values near streams in the basin might indicate fast recharge from channel leakage, and that low tritium values in other wells away from streams indicate a slow component of groundwater movement. Furthermore, since low tritium values were generally found throughout the Principal Aquifer, the slow movement of groundwater may be of greater significance than previously recognized.

Geology and Occurrence of Groundwater

A geologic column is shown in Table I. For details, we refer the reader to the work by Kelley (1971) and Gross et al. (1976).

The Yeso Formation of Permian age is the oldest water-bearing unit considered in this study. It is composed of sandstone, shale, anhydrite, limestone and salt. The formation crops out along the southwest slope of the Sacramento Mountains, and is also found in the river valleys which have cut the eastern slope of these mountains. The Yeso ranges in thickness from 1000 to 2000 feet in the western part of the basin.

As an aquifer the Yeso yields small to moderate quantities of water; the quality is generally poor but suitable for stock use. The Yeso receives most of its recharge from infiltration through overlying beds as well as by stream leakage in the alluvial valleys. The permeability of this unit is thought to be low but of sufficient degree to allow transport down the dip of the eastern slope.

The Glorieta Sandstone of late Permian age is the basal member of the San Andres Formation. The unit is composed of fine-grained, well-sorted, friable sand and is easily distinguished from the red-brown Yeso by its yellow color. Outcrops are visible along the valleys and canyons which cut the east slope of the Sacramento Mountains within the study area.

Wells in the Glorieta aquifer yield a moderate quantity of water. Water quality is good where the aquifer is recharged by

Table I. Simplified Stratigraphic Column for the Roswell Basin.

AGE	GROUPS, FORMATIONS, MEMBERS	DESCRIPTION
Holocene and Pleistocene	Alluvium	0-300 ft. thick Caliche, gravels, sands some clays.
Pleistocene and Pliocene	Gatuna formation	0-250 ft. thick Sands, clays, gravels, red color, thin layers of carbonates.
Permian	Artesia group Tansill formation Yates formation Seven Rivers formation Queen formation Grayburg formation	0-400 ft. thick Upper portion: Clays, sands, evaporites. Lower portion: Clays, sands, carbonates. The Queen formation is usually considered to form the aquitard.
	San Andres formation Fourmile Draw member Bonney Canyon member Rio Bonito member Glorieta sandstone	200-? ft. thick Upper portion: Evaporites, sands (Lovington sandstone), carbonates. Lower portion: Carbonates, sands (Glorieta sandstone), shales.
	Yeso formation	

Precambrian

precipitation or channel leakage, but poor quality water is found where it is supplied by the lower Yeso Formation.

The San Andres Limestone crops out extensively in the Roswell basin. Within the study area the formation is above the regional water table, but perched groundwater is apparent from springs which discharge above major streams. Although the San Andres has been characterized as a highly permeable unit, large differences in hydraulic conductivity and porosity exist. These differences may be explained by the variability of occurrence of solution openings and fracturing. The dissolution of limestone is most intense along major lines of drainage where interconnection of groundwater and surface water is possible. The Border Hills structure trending northeast in the western part of the study area, has little effect on groundwater movement across the basin. However, fracturing along this structure may influence the quantity of recharge made available to the water table. While the San Andres Formation is not an aquifer in the area of this study, it does have an important role with respect to recharge of the Yeso and Glorieta aquifers.

Ten observation wells were drilled and completed by the Pecos Valley Artesian Conservancy District in 1957. These wells were equipped with recording devices, and nearly continuous water level data for most of the wells are available from 1958 to present. The drilling of these wells was the result of a report by M. S. Hantush (1957), to provide information on the groundwater conditions of the Roswell basin. Lithologic logs and water levels can be found in State Engineer Report No. 16 (Crawford and Borton, 1958). Location of these wells and others used in this report is found in Figure 2.

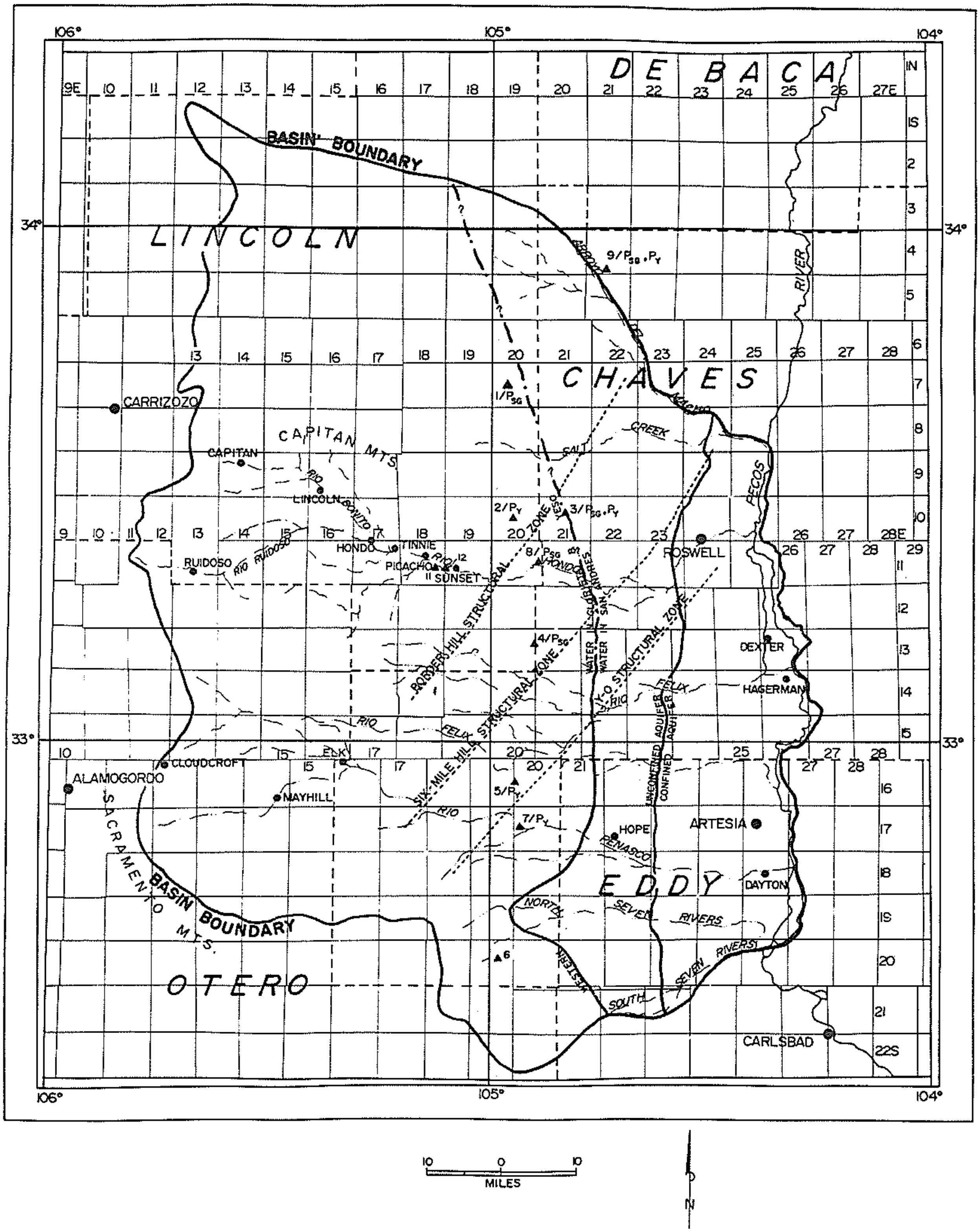

Fig. 2: Location of wells and hydrologic boundaries. Triangles: observation wells. No. 10, not shown, is outside of the area of interest. Nos. 5, 6 and 10 are no longer maintained and were not used. Main water-producing formations: P_{SG} = Glorieta Sandstone; P_Y = Yeso Formation. Cf. Table I.

Drainage

The Rio Hondo and the Rio Peñasco drainage originate in the Sacramento Mountains and flow east to the Pecos River. The Hondo is formed by the confluence of Rio Bonito and Rio Ruidoso at Hondo, New Mexico. Near the junction, the Hondo is perennial but loses most of its flow to seepage, irrigation and evaporation along the rest of its course. The Bonito and Ruidoso are perennial over much of their course, except for a few places where the flow is lost to irrigation, diversion, and seepage. A water table map constructed by Mourant (1963) gives evidence of channel leakage and groundwater mounding under some sections of the Hondo drainage. This is particularly evident in the central and eastern part of the study area. Similar to the Hondo, the Rio Peñasco drainage loses most of its flow between Elk and Dayton.

Hydraulic connection between the stream and aquifer has been observed in the Hondo and Peñasco drainages. Where the water table is at or near the level of the stream, pumping for irrigation will lower the water table causing an increase in channel leakage and a loss in streamflow. Along the drainages of the Peñasco and the Hondo, deep wells 100 to 500 feet below the stream display large fluctuations which appear to correspond to changes in stream discharge. The present report examines this response in detail.

Other streams, arroyos and channels in the basin are very likely controlled by similar mechanisms. However, information and data are more complete in the Hondo and Peñasco drainages, and are used in this report.

Rainfall-Runoff in the Basin

In this subsection, a brief description is given of rainfall-runoff in the study area and the importance of this process to recharge. Figure 3 gives the location of stream gauges maintained by the U. S. Geological Survey in the basin. Some of the gauges have been discontinued. In these cases only partial records are available. The gauges of primary importance to this study are: No. 3901 at Picacho, No. 3905 at Diamond 'A' Ranch and No. 3985 at Dayton. The data from these gauges are tabulated in Appendix A.

The major streams in the basin can generally be described as perennial in the headwaters and ephemeral (flow in response to rainfall) in the central and eastern parts of the basin. There are also sections of the Peñasco, Felix and Hondo rivers which can be classified as intermittent; they flow in response to seasonal sources such as snowmelt or springs.

Mean areal precipitation has been estimated by Gross et al. (1976) using Thiessen polygons. An average figure for mean annual precipitation over the 8200 square mile area of the basin is on the order of 5.5×10^6 acre-feet. From 4 to 8% of this quantity is assumed to be recharge to the groundwater basin (Saleem and Jacob, 1971). Since reliable information on areal precipitation and recharge has not been developed for the basin, precise estimates can not be given. The mechanisms which control recharge are among the unknown quantities in the hydrologic cycle of this region.

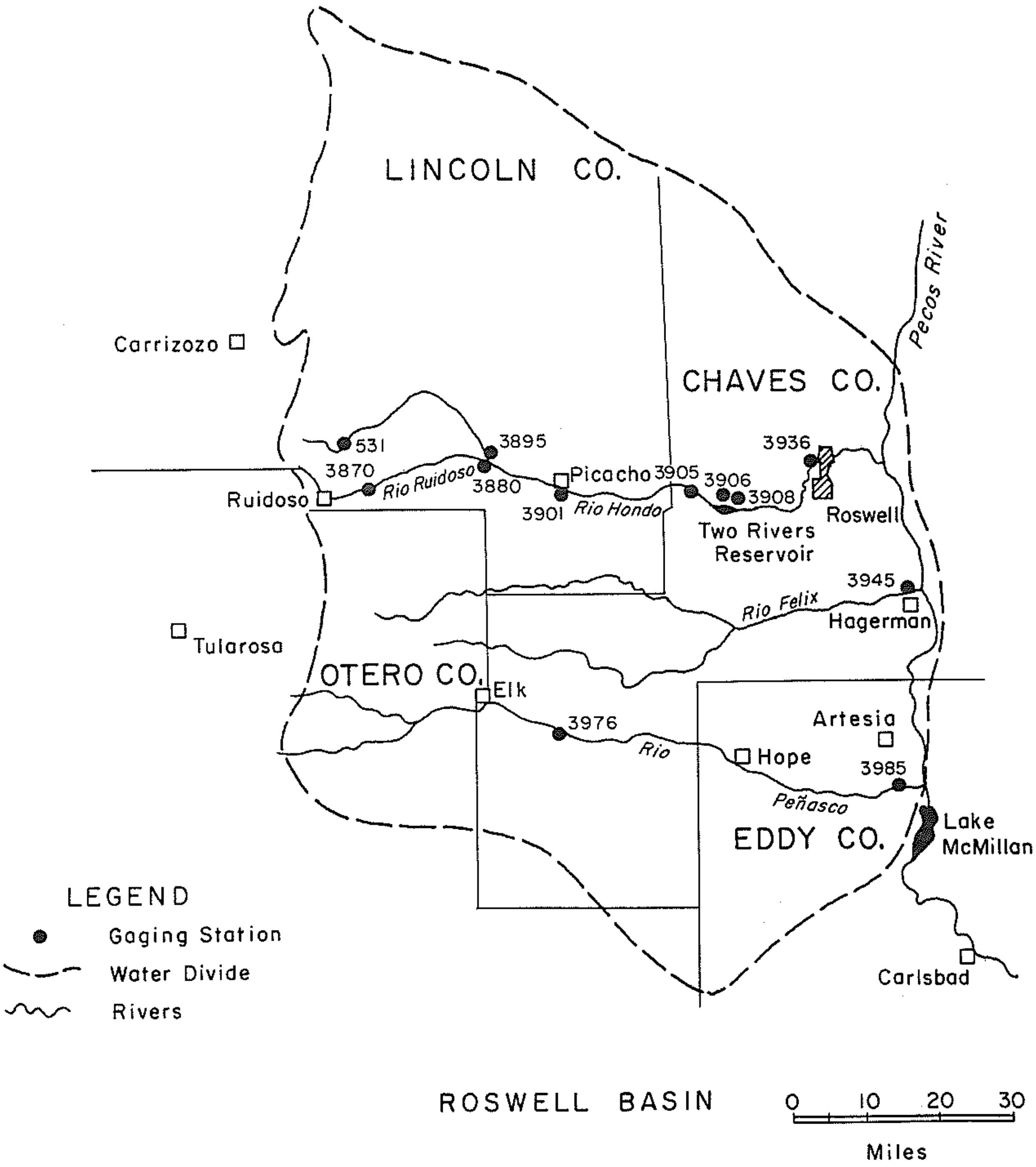

Fig. 3: Location of stream gauges.

A simple method of describing the relationship between rainfall and runoff is to plot rainfall versus stream discharge. Linear regression between the variables gives an indication if streamflow is directly affected by precipitation.

Rainfall records at Picacho and discharge at Diamond 'A' Ranch were used since long records are available for both stations (the period used was 1959-1975). Linear regression of monthly mean precipitation at Picacho and monthly mean discharge at Diamond 'A' Ranch had a correlation coefficient of 0.50. Using an F-test the correlation proves to be significant, but only explains 50% of the variation. Evidently the direct relationship between monthly rainfall and runoff does not adequately describe the process. Harmonic analysis would very likely indicate the indirect, or lagged, relationship between rainfall and runoff.

Section 2

EXAMINATION OF GROUNDWATER AND SURFACE WATER DATA

Objective

In this section we examine available hydrologic data in the study region and evaluate possible recharge mechanisms. The grouping of wells according to water level response is the first objective. The water level response is then associated with some type of input such as precipitation and/or stream flow. The use of tritium as a tracer in the hydrologic cycle is examined as an indication of the source of recharge to the groundwater system.

Groundwater Level Response

Groundwater level fluctuations have been used by many investigators to analyze the mechanism of recharge. C. E. Jacob (1944) correlated precipitation with groundwater levels on Long Island, New York. A more recent paper by C. Venetis (1970) presents a different approach by treating the water level changes themselves as indicators of groundwater recharge or discharge. The purpose of this section is to analyze the characteristics of water level changes in several wells in the study region to determine the cause of these changes and their relationship to recharge.

Continuous well level data were obtained from the Pecos Valley Artesian Conservancy District for seven observation wells maintained by their office (Nos. 1, 2, 3, 4, 7, 8, and 9 of Fig. 4 and Appendix A). Because of the size of the study area, the sparsity of wells, and the inherent sampling errors, monthly average water levels were deemed sufficient to characterize the flow system.

A reasonable way to establish the mechanism of recharge in a particular hydrologic system is to associate groundwater level changes with some causal variable or group of variables. Statistical methods and harmonic analysis are often used to illustrate linear or cyclic behavior of hydrologic data. A simpler and more direct approach is a graphical representation and comparison of input and output variables.

A graphical examination of monthly average groundwater levels in the study area indicated essentially two different responses. The first group of wells (Nos. 1, 2, 3, 4, 9) displayed a long trend of decreasing water levels from 1958-1971, with a much faster recovery from 1972-1976. This group of wells was located away from major lines of drainage. The second group (Nos. 7, 8) exhibited a widely fluctuating cyclic behavior. This response was typical of wells located near streams or arroyos. Well No. 4 exhibits cyclic fluctuations superposed on a long-term trend.

Long-Term Response Wells

Figure 4 shows the wells with a long-term water level response. A surprising absence of seasonal or annual fluctuations is readily apparent for wells No. 2 and No. 3. These wells are located on the west and east side, respectively, of the Border Hills structure north of Highway 380. The principal water-bearing formation of these wells is the Yeso (Gross, et al., 1976, Appendix B). However, some water was encountered in the Glorieta at both wells. Observation well No. 4 displays some fluctuation indicating seasonal recharge. Despite the higher frequency fluctuations in No. 4 the long-term response to recharge and discharge is similar to No. 2 and No. 3.

The long-term changes in water level indicate a damped system. Typically, a system of this type shows little or no changes in storage from a single input (seasonal rainfall or snowmelt) while a series of closely spaced inputs would contribute substantially to groundwater storage. Precipitation in the Roswell basin for the years 1959-1970 was generally below the long-term mean, while rainfall from 1971-1976 was generally above the mean. The distribution of rainfall in time evidently is an important consideration for recharge from areal precipitation. It is also interesting to note that pumpage from the Artesian basin is inversely related to rainfall. During wet years, less aquifer withdrawals are necessary and vice versa. Long-term trends of water levels in the recharge

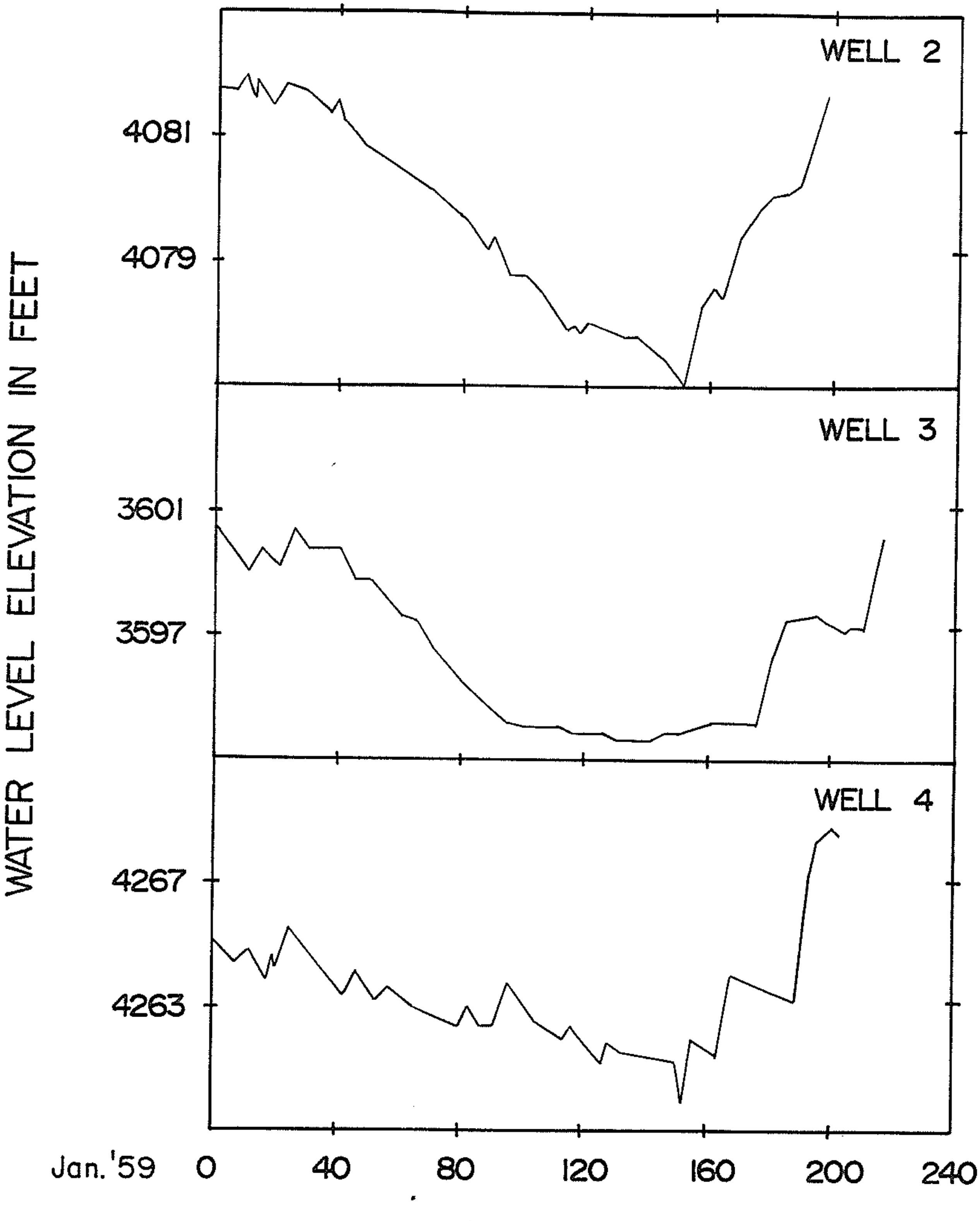

Fig. 4: Long-term response wells. Well No. 4 exhibits cyclic fluctuations superposed on a long-term trend.

area are closely tied to this recharge/discharge (basin pumpage) relation.

A qualitative description of the areal rainfall/recharge process is not an adequate tool for water management in a large groundwater basin. The long-term response of water levels to recharge from precipitation should be studied in detail to establish physically based relationships. Perched groundwater systems which discharge water from springs in the recharge area may give information on the relation between areal rainfall and recharge.

Fast Response Wells

The second type of well response is shown in Figure 5. These wells show a definite effect from short-term or seasonal inputs. Well No. 8 is located about 1000 feet north of the Rio Hondo at Diamond 'A' Ranch while No. 7 is located approximately 500 feet north of the channel of the Rio Peñasco. The water level changes in these two wells are thought to be related to changes in streamflow, that is, channel leakage.

Two additional fast-response wells (Nos. 11 and 12) are discussed in Section 3 of this report.

The response in these wells appears to be less damped than in the wells examined previously. Nonetheless, the comparison of streamflow events with water level fluctuations, to be discussed below, indicates that extended periods of above-average streamflow (as opposed to sporadic floods) are required to produce appreciable water level fluctuations, the large amplitude of which may be accounted for by the intense concentration of recharge along major channels.

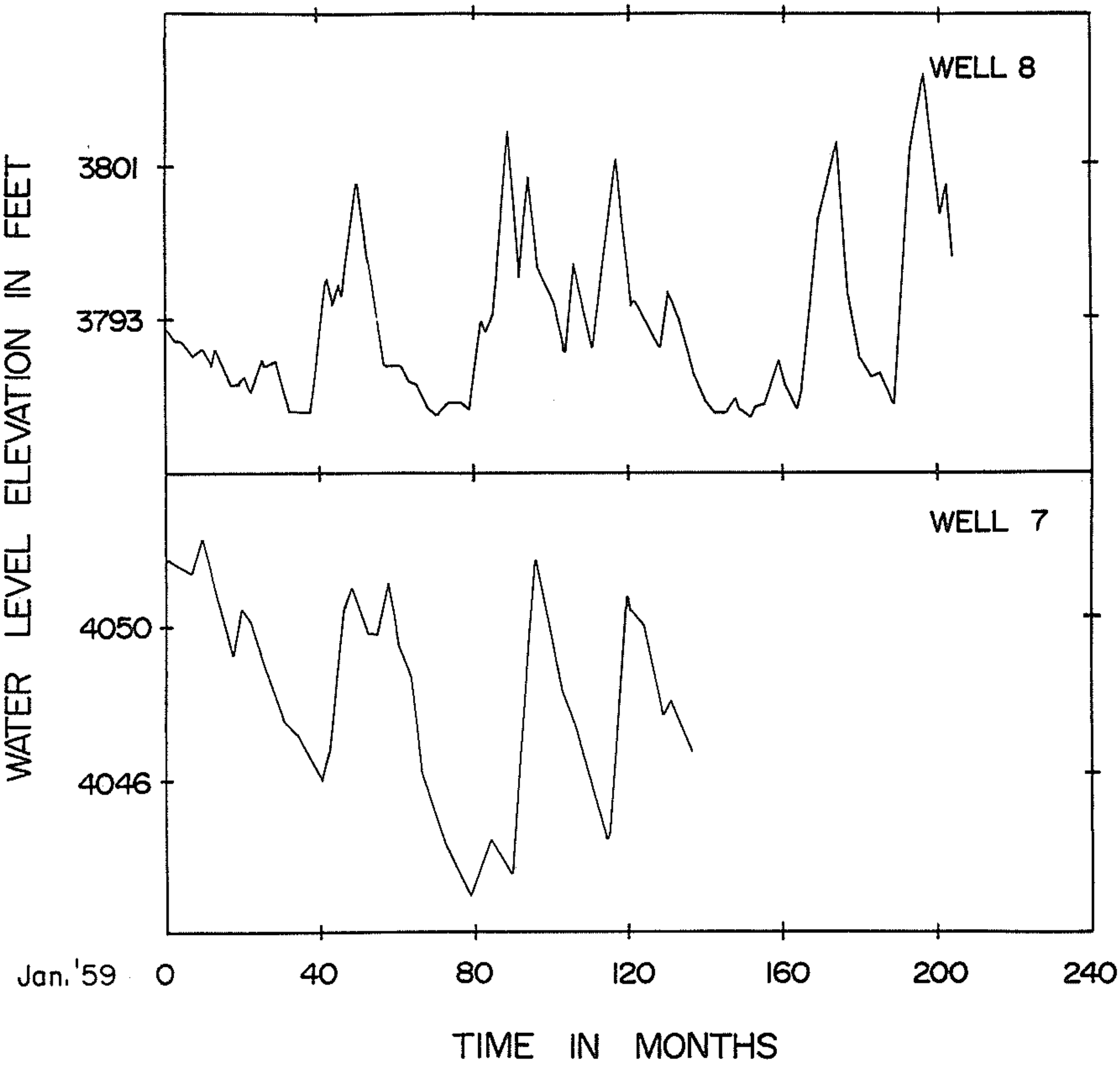

Fig. 5: Fast-response wells.

Groundwater Recharge from Channel Leakage

It has been found by several investigators that channel leakage to the groundwater reservoir in the basin is considerable. Fiedler and Nye (1933) observed that stream losses from the Rio Hondo and Rio Peñasco were greater where these streams cross the Principal Intake Area. They also noted that above the Diamond 'A' Ranch headquarters the Rio Hondo normally flows, while between the Diamond 'A' headquarters and Hondo Reservoir the entire flow sinks into the limestone. The Rio Peñasco will normally flow at Elk while the stream gauge at Dayton (3985) has flow only after large precipitation events. Bean (1949) has estimated channel losses to be on the order of 19,000 ac-ft annually for the Hondo, and 9,000 ac-ft annually for the Peñasco.

Several physical factors influence channel leakage. In the study area, along the western flank of the basin, vertical infiltration in the river valleys occurs through a permeable alluvial deposit, or directly through the limestone. Where the water table is below the stream, a large storage capacity for recharge exists. Along the valleys of the Peñasco and the Hondo irrigation water is supplied by the stream. The quantity of water applied to crops in excess of consumptive use will infiltrate the alluvium as recharge or be returned to the stream. Irrigation, domestic and stock wells along these valleys have the effect of lowering groundwater levels and increasing the storage capacity of the groundwater reservoir.

For an initial estimate of the amount of channel leakage from the Rio Hondo west of the Principal Intake Area of Fiedler and Nye and in the study area for this report, mean monthly discharge for two gauging stations was plotted and compared using linear regression. The upstream gauge was located at Picacho (No. 3901), and the downstream gauge at the Diamond 'A' Ranch (No. 3905). The stations are approximately 17 miles apart. Both stations are affected by upstream irrigation. Two irrigation ditches above the Picacho gauge reduce discharge at Picacho while a portion of the flow is returned below the gauge. The measurements from these gauges are tabulated in Appendix A.

A runoff plot between the two gauges is given in Figure 6. The Diamond 'A' discharge is the independent variable, x_i, and Picacho discharge is the dependent variable, y_i. From the regression equation

$$y_i = \beta_1 x_i + \beta_0 \quad ,$$

it was found that the intercept, $\beta_0 = 7.61$ and the slope $\beta_1 = 1.04$. The correlation coefficient was found to be 0.98. The intercept can be thought of as an estimate of the loss between the gauges. Initial estimates of channel loss for this section of the Hondo are calculated to be 220 ft^3/month per foot of channel.

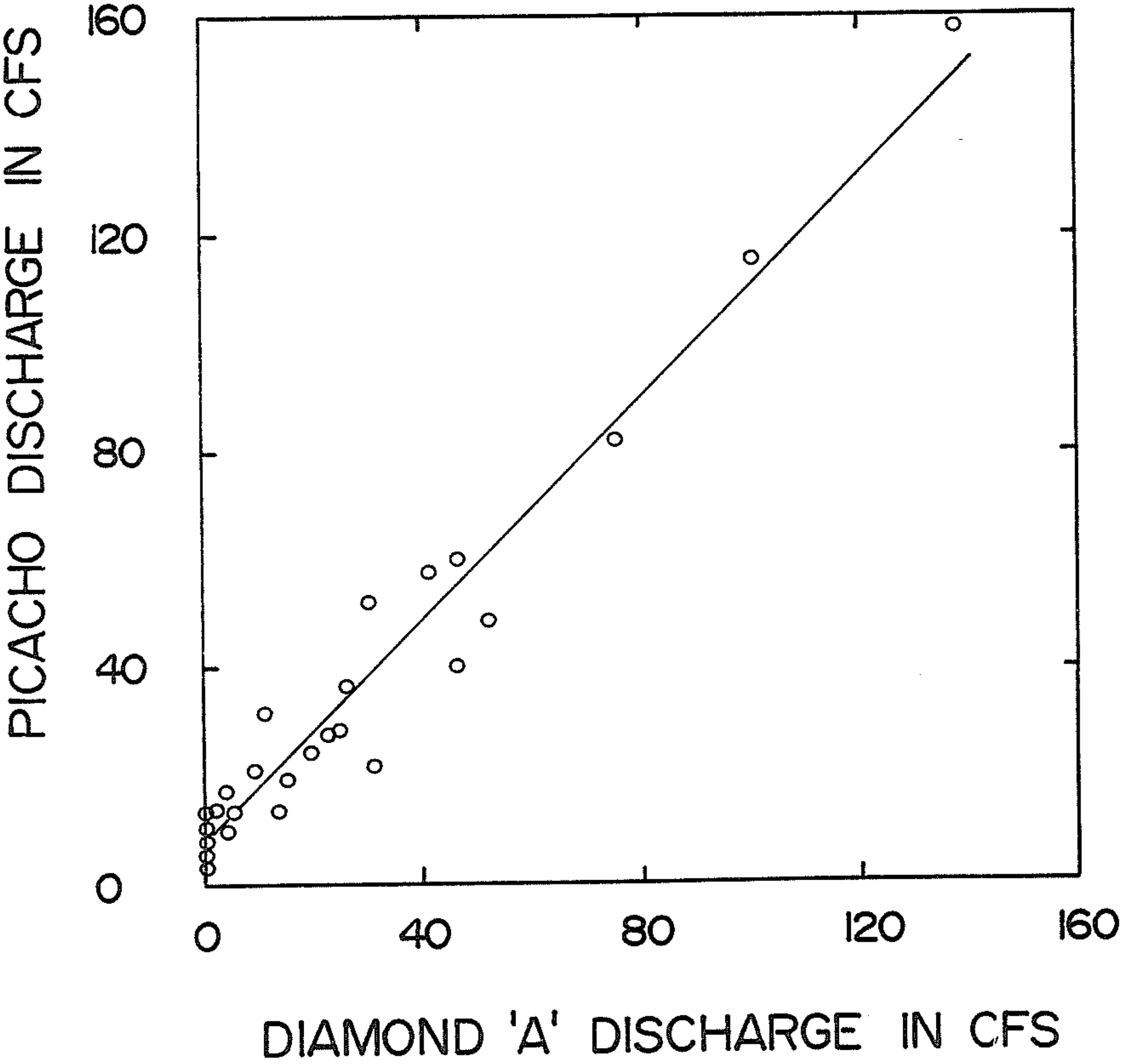

Fig. 6: Regression between Picacho and Diamond 'A' gauges.

Tritium as a Recharge Indicator

Environmental tritium is useful as a tracer in the hydrologic cycle. The method was applied to regional flow in the Roswell basin by Rabinowitz and Gross (1972). Tritium (H^3) has been introduced to the hydrologic cycle by atmospheric nuclear testing. The application to hydrology stems from the fact that pulses of tritium from seasonal precipitation eventually reach the surface water and groundwater reservoirs. Since the half-life of tritium is 12.4 years (Jacobs, 1968, p. 4) an estimate of the 'age' of a particular sample can be inferred if that age is comparable to the half-life. Tritium values for surface water in the Rio Hondo drainage are typically high (>20 tritium units - see Gross et al., 1976). Several wells (Nos. 8, 11, 12) near the Hondo also show consistently high values of tritium. However, other wells (Nos. 2, 3, 4), from 5 to 10 miles north and south of the drainage, are consistently low. The fact that the Rio Hondo loses flow to the groundwater has long been known and is supported by tritium sampling.

Water samples from the Rio Peñasco near Elk are usually low in tritium. Exceptions to this are noticed during high runoff periods, caused by recent rainfall or snowmelt. The typical low values (<15 tritium units) are probably explained by the many springs in the area which discharge 'older' water from perched systems, or from groundwater baseflow. Groundwater samples taken from observation well No. 7, near the Rio Peñasco, are generally low in tritium.

Channel leakage and groundwater recharge from the river could not be confirmed using tritium. Table II includes the tritium data of surface water and well samples used in the study. The tritium analyses were made at New Mexico Institute of Mining and Technology.

Table II. Tritium Values of Surface Water and Wells.

1. Rivers

Date	Location	Concentration (T.U.)
1/ 1/73	Rio Hondo 2 miles east of Hondo (11.17.11.300)	71.2
5/26/73	Rio Hondo 2 miles east of Tinnie (11.18.07.000)	83.3
10/1/76	Rio Hondo at Picacho (11.18.00.000) (near well #11)	29.6
5/27/73	Rio Ruidoso at Hondo (11.17.05.000)	43.1
3/24/74		50.9
8/12/74		31.6
12/16/74		37.6
3/26/75		60.0
6/10/75		52.2
8/26/76		46.5
10/ 1/76		40.1
7/10/73	Rio Bonito at Fort Stanton	68.0
3/26/75		77.1
6/10/75		13.4
8/26/75		63.0
10/ 4/75		57.3

1. Rivers continued

Date	Location	Concentration (T.U.)
1/ 1/73	Rio Bonito at Baca Campground (9.15.14.240)	119.0
7/10/73		95.7
6/12/74		17.3
12/16/74		33.0
3/26/75		63.0
6/10/75		75.8
8/26/75		28.9
10/ 4/75		33.2
5/27/73	Rio Bonito at Hondo (11.17.05.000)	43.1
3/24/74		50.9
6/12/74		31.6
12/16/74		37.7
3/26/75		60.0
6/10/75		52.2
8/26/75		46.5
12/19/74	Rio Peñasco 13 miles east of Elk on U.S. 82, south of highway (17.20.18.434)	5.8
3/28/75		15.2
8/28/75		14.4
7/11/73	Rio Peñasco 3 miles east of Elk on U.S. 82 (16.16.11.240)	27.8
4/ 8/74		8.7
12/19/74		9.8
2/21/75		9.4
8/28/75		15.3

Table II. Continued.

2. Wells near the Rio Peñasco or Rio Hondo		
Date	Location	Concentration (T.U.)
3/22/74	Well #8 18 miles west of Roswell on U.S. 380 at Diamond 'A' Ranch (1000' north of Hondo) (11.21.18.333)	58.7
6/13/74		43.7
8/26/74		49.2
12/17/74		43.6
3/27/75		47.1
8/26/75		50.8
10/ 1/76	Well #11 R. O. Anderson well near Picacho (11.18.16.444)	31.8
10/ 1/76		32.6
10/ 2/76	Well #12 R. O. Anderson well near Picacho (11.18.24.341)	28.8
4/ 8/74	Well #7 13 miles east of Elk on U.S. 82, south of highway (17.20.18.434)	12.9
12/19/74		4.0

3. Wells located away from major surface drainages		
Date	Location	Concentration (T.U.)
4/10/74	Well #1 (7.20.16.333)	3.5
9/20/75		12.8
3/22/74	Well #2 (10.20.16.444)	40.8
6/12/74		3.4
8/26/74		3.0
12/17/74		1.3
3/27/75		8.8
8/26/75		8.7
12/16/74	Well #3 (10.21.16.222)	0.6
3/27/75		5.4
8/26/75		4.8
3/22/74	Well #4 (13.20.13.222	2.7
6/13/74		10.5
8/25/74		1.7
12/17/74		0.0
3/28/75		2.5
8/27/75		9.2
3/23/74	Well #9 (4.21.33.111)	24.4
6/13/74		3.6
8/25/74		2.2
12/18/74		2.8
3/27/75		8.3
10/ 4/75		5.7

Section 3

A STOCHASTIC STREAM-AQUIFER MODEL

Objective

The purpose of this section is to estimate aquifer parameters and to evaluate a recharge mechanism in the western region of the Roswell basin. Although a great deal of work has been devoted to the hydrology and hydrogeology of the Roswell basin proper, little quantitative information is available about the water resources of the Yeso, Glorieta and Alluvial aquifers of its western flank; their relative importance as a groundwater reservoir is not well established.

The interpretation of fluctuating water levels by mathematical models has been attempted by several investigators. Jacob (1943) and Venetis (1971) have already been mentioned. Cooper and Rorabaugh (1963) and Hall and Moench (1972) also investigated aquifer models of this type. A deterministic approach was used for the above models. Gelhar (1974) developed three analytical models which describe the spectral response of water table aquifers. The first and simplest case is a linear reservoir, lumped parameter model. The second is a linearized form of the Dupuit model, and the third is a Laplace type aquifer model. The stochastic models proposed by Gelhar describe the spectral response of groundwater levels to recharge and to changes in adjacent stream depth. In this paper the groundwork is laid for applications of stochastic analysis to a phreatic aquifer.

The analysis of hydrologic time series using a stochastic approach has been shown to be useful where complicated physical phenomena appear to be dominated by a random element. This random element may be associated with the space or time variability of a series. This study is concerned with the randomness of water level and streamflow time series, and their spectral representation in the frequency domain. A stochastic description rather than the conventional deterministic approach implies that sequences of hydrologic events are characterized by probability laws.

In this study time changes of groundwater levels and stream discharge are regarded as stochastic processes and then modeled as a stream-aquifer system. By treating the time series of streamflow (input) and water level (output) as random processes, it is possible to describe the input-output relationship in terms of the individual spectra. The usefulness of this approach is that the aquifer parameters, hydraulic conductivity and effective porosity, can be estimated and values for recharge to the groundwater system can be inferred. A detailed description of the mathematics of spectral representations of time series is found in Jenkins and Watts (1968).

A General Two Dimensional Model

The partial differential equation of groundwater flow for a water table aquifer in two dimensions can be written as

$$S \frac{\partial h}{\partial t} = \frac{\partial}{\partial x}\left(K_x h \frac{\partial h}{\partial x}\right) + \frac{\partial}{\partial y}\left(K_y h \frac{\partial h}{\partial y}\right) + E(x,y,t) \quad , \tag{1}$$

where K_x and K_y are hydraulic conductivities in the x,y directions, h(x,y,t) is the hydraulic head, S is the storage coefficient or effective porosity, and E(x,y,t) is the recharge rate to the aquifer. To linearize Eq. (1) assume $K_x = K_y = K$ and $K\bar{h} = T$ or transmissivity. The term $\bar{h}$ denotes an average value of hydraulic head. As long as changes in h(x,y,t) are small compared to the thickness of the aquifer, the effect of assuming a constant transmissivity will be negligible. For simplicity, the assumptions that S is a constant and E is independent of the distance y along the stream is made. Eq. (1) is now written as

$$S \frac{\partial h}{\partial t} = T \frac{\partial^2 h}{\partial x^2} + T \frac{\partial^2 h}{\partial y^2} + E(x,t) \quad . \tag{2}$$

In the study area it is known that losing streams contribute recharge to the deep water table. Figure 7 is a schematic of this process. The inflow E is handled as a Dirac delta function δ(x) at x = 0. It can be thought of as a line source of recharge in the direction of the stream, such that E(x,t) = q(t)δ(x). If the regional water table gradient ∂h/∂y is approximately constant, its derivative vanishes, and Eq. (2) is further simplified to

$$S \frac{\partial h}{\partial t} = T \frac{\partial^2 h}{\partial x^2} + q(t)\delta(x) \quad , \tag{3}$$

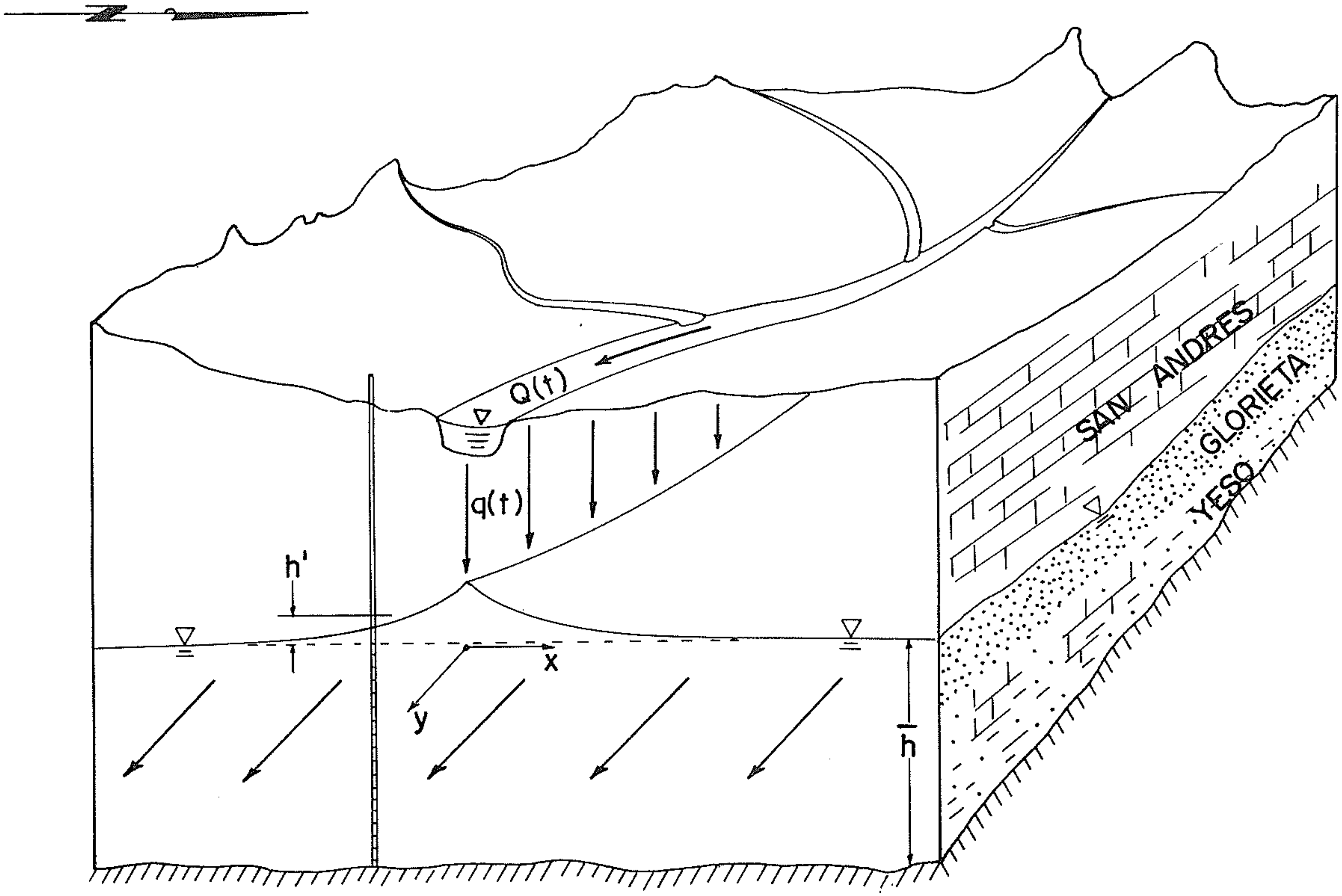

Fig. 7: Model of a stream losing to an aquifer.

which represents the governing flow equation for the proposed model. Integration of (3) over a small interval (-Δx, Δx) results in the boundary condition

$$2T \frac{\partial h}{\partial x} \bigg|_{x=0} = -q(t) \quad , \tag{4}$$

where q(t) is the recharge rate from the stream. A linear relationship is assumed between stream discharge Q(t) and recharge q(t)

$$q(t) = a\,Q(t) \quad , \tag{5}$$

where the parameter <u>a</u> is a constant fraction of discharge representing the amount of channel loss to the aquifer. The effect of the unsaturated zone is not explicitly taken into account in the proposed model.

Spectral Representation of the Model

To apply the properties of a stationary random process to the water level and recharge series, it is necessary to describe them in terms of mean values $\bar{h}$, $\bar{q}$, and the fluctuations about the mean, h', q', such that

$$\begin{aligned} h &= \bar{h} + h' \\ q &= \bar{q} + q' \quad . \end{aligned} \tag{6}$$

Figure 8 demonstrates the separation of the mean and the fluctuations about the mean for a single water level series. The differential equation of the mean values is

$$T \frac{\partial^2 \bar{h}}{\partial x^2} + \bar{q}\ \delta(x) = 0 \quad . \tag{7}$$

By substitution of Eq. (6) into the original differential Eq. (3) and subtracting the differential equation of the mean Eq. (7), a new equation is derived which governs the fluctuations about the mean

$$S \frac{\partial h'}{\partial t} = T \frac{\partial^2 h'}{\partial x^2} + q'\ \delta(x) \tag{8}$$

with boundary conditions

$$2T \frac{\partial h}{\partial x} \bigg|_{x=0} = -q' = -a\ Q'(t) \quad . \tag{9}$$

The stream discharge $Q'(t)$ is also represented as a zero mean random process.

From the representation theorem of Fourier time series analysis (Lumley and Panofsky, 1964, p. 16), a random stationary process

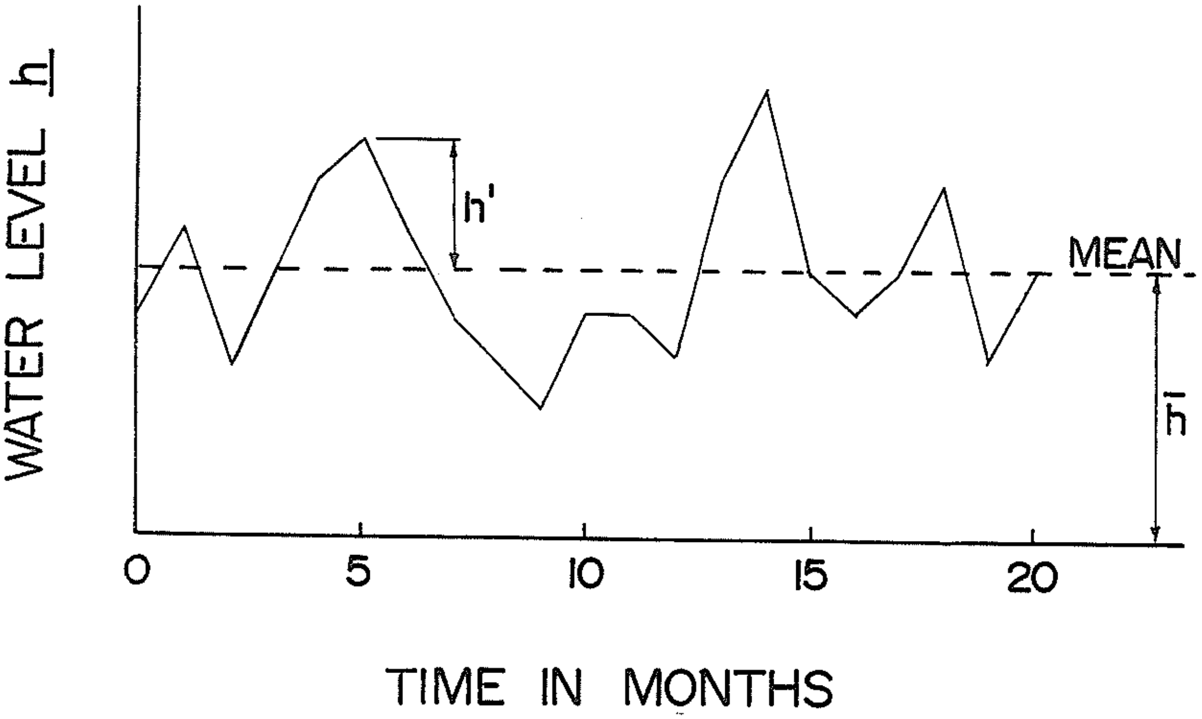

Fig. 8: Water level fluctuations about the mean.

can be described by a stochastic Fourier-Stieltjes integral

$$h'(x,t) = \int_{-\infty}^{\infty} e^{i\omega t}\, dZ_h(\omega,x) \tag{10}$$

$$Q'(t) = \int_{-\infty}^{\infty} e^{i\omega t}\, dZ_Q(\omega) \tag{11}$$

where ω is angular frequency and dZ_h, dZ_Q are the Fourier amplitudes of the process which have the following properties

$$E\left[dZ_h(\omega_1,x) \cdot dZ_h^*(\omega_2,x)\right] = \begin{cases} 0 \;, & \omega_1 \neq \omega_2 \\ \phi_{hh}(\omega,x)d\omega \;, & \omega_1 = \omega_2 \end{cases} \tag{12}$$

The asterisk indicates complex conjugate and $\phi_{hh}(\omega,x)$ is the spectral density function of $h'(x,t)$. Substituting Eqs. (10) and (11) into Eq. (8), a solution in terms of the Fourier amplitudes is found

$$dZ_h(\omega,x) = \frac{dZ_Q(\omega)a}{2T}\left(\frac{T}{i\omega S}\right)^{\frac{1}{2}} \exp\left[-\left(\frac{i\omega S}{T}\right)^{\frac{1}{2}} x\right] \;. \tag{13}$$

From the properties of Eq. (12) the spectral density for the output of the system can be written

$$\phi_{hh}(\omega,x) = \frac{\phi_{QQ}a^2}{4\omega ST} \exp\left[-x\left(\frac{2\omega S}{T}\right)^{\frac{1}{2}}\right] \tag{14}$$

The result in Eq. (14) describes the input-output relationship of recharge and water level in terms of their individual spectra. The parameter x is distance from the well to the stream and a is the stream leakage parameter.

Following the same approach the cross-spectrum ϕ_{Qh} can be found from

$$E\left[dZ_Q(\omega_1) \cdot dZ_h^*(\omega_2,x)\right] = \begin{cases} 0 \ , \ \omega_1 \neq \omega_2 \\ \phi_{Qh}(\omega,x)d\omega \ , \ \omega_1 = \omega_2 \end{cases} , \quad (15)$$

and the cross spectrum becomes

$$\phi_{Qh}(\omega,x) = \phi_{QQ}(\omega) \cdot B \exp\left[-\frac{\sqrt{2}}{2}\alpha + i\left(\frac{\sqrt{2}}{2}\alpha + \frac{\pi}{4}\right)\right] \quad (16)$$

where

$$B = \frac{a}{2T}\left(\frac{T}{\omega S}\right)^{\frac{1}{2}} \text{ and } \alpha = x\left(\frac{\omega S}{T}\right)^{\frac{1}{2}} . \quad (17)$$

The spectral density function or spectrum $\phi(\omega)$ of $h'(x,t)$ and $q'(t)$ is related to the autocovariance function $R(\tau)$ by the Fourier transform and inverse transform respectively

$$R_{hh}(\tau) = \int_{-\infty}^{\infty} e^{i\omega\tau} \phi_{hh}(\omega,x)d\omega \quad (18)$$

$$\phi_{hh}(\omega,x) = \frac{1}{2\pi}\int_{-\infty}^{\infty} e^{-i\omega\tau} R_{hh}(\tau)d\tau . \quad (19)$$

In the same sense the cross spectral density function $\phi_{Qh}(\omega,x)$ is related to the cross-covariance function $R_{Qh}(\tau)$ by its Fourier transform and inverse transform

$$R_{Qh}(\tau) = \int_{-\infty}^{\infty} e^{i\omega\tau} \phi_{Qh}(\omega,x)d\omega \quad (20)$$

$$\phi_{Qh}(\omega,x) = \frac{1}{2\pi}\int_{-\infty}^{\infty} e^{-i\omega\tau} R_{Qh}(\tau)d\tau . \quad (21)$$

The autocovariance and cross-covariance are only functions of τ, the time differences or lag. This results from the property of stationarity in time series. If the autocovariance of a particular time series is independent of time, the process is said to be stationary, and spectral analysis is applicable. A more detailed discussion of this property of time series analysis and its implications is given in Appendix A.

It is often convenient to define the input-output spectrum using ordinary frequency, f, (cycles/time interval), where $\omega = 2\pi f$. The spectral relationship between head and stream leakage in terms of f is then given by

$$\frac{\phi_{hh}(f,x)}{\phi_{QQ}(f)} = \frac{a^2}{8\pi f S T} \exp\left[-x\left(4\pi f \frac{S}{T}\right)^{\frac{1}{2}}\right] , \tag{22}$$

and the cross-spectrum is

$$\frac{\phi_{Qh}(f,x)}{\phi_{QQ}(f,x)} = B \exp\left[-\frac{\sqrt{2}}{2}\alpha + i\left(\frac{\sqrt{2}}{2}\alpha + \frac{\pi}{4}\right)\right] \tag{23}$$

where

$$B = \frac{a}{2T}\left(\frac{T}{2\pi f S}\right)^{\frac{1}{2}} \quad \text{and} \quad \alpha = x\left(2\pi f \frac{S}{T}\right)^{\frac{1}{2}} . \tag{24}$$

For ease of presentation all equations have been derived in continuous form. Discrete representations for the spectral estimators $\hat{\phi}_{QQ}$ and $\hat{\phi}_{hh}$, as well as the covariance estimators $\hat{R}_{hh}(\tau)$, $\hat{R}_{QQ}(\tau)$, $\hat{R}_{Qh}(\tau)$, were accomplished using the U.C.L.A. biomedical computer program BMDO2T (Dixon, 1976).

Phase Relationship or Lag Property

The cross-spectrum of a bivariate random process $[h'(x,t), Q'(t)]$ leads to another useful aspect of time series analysis, the phase spectrum $\theta_{Qh}(f,x)$ or, simply, the phase. It demonstrates the time lag between the frequency components of the two processes $h'(x,t)$ and $Q'(t)$. The cross-spectrum can be written

$$\phi_{Qh} = A_{Qh} \exp \left[i\theta_{Qh}\right] \tag{25}$$

where A_{Qh} is the amplitude spectrum and θ_{Qh} is the phase (Jenkins and Watts, p. 347). The cross-spectrum Eq. (23) of this analysis in the general form given by Eq. (25) is

$$\phi_{Qh} = \phi_{QQ} B \exp \left[-\frac{\sqrt{2}}{2}\alpha\right] \exp \left[i\left(\frac{\sqrt{2}}{2}\alpha + \frac{\pi}{4}\right)\right] \tag{26}$$

where

$$B = \frac{a}{2T}\left[\frac{T}{2\pi fS}\right]^{\frac{1}{2}} \quad \text{and} \quad \alpha = x\left[2\pi f \frac{S}{T}\right]^{\frac{1}{2}} \quad .$$

The argument of the complex function in Eq. (26) is the phase in radians.

$$\theta_{Qh} = x\left(\pi\frac{S}{T}\right)^{\frac{1}{2}} f^{\frac{1}{2}} + \frac{\pi}{4} \quad . \tag{27}$$

Estimation of Aquifer Parameters and Recharge

If the process of recharge from a losing stream to the aquifer is represented by the proposed model, the spectral relationship of Eq. (22) should be linear in $\ell n\left[f(\hat{\phi}_{hh}/\hat{\phi}_{QQ})\right]$ and $f^{\frac{1}{2}}$, the dependent and independent variable, respectively. Eq. (22) can be written

$$\ell n\left[f\ \frac{\hat{\phi}_{hh}}{\hat{\phi}_{QQ}}\right] = -\beta_1\ f^{\frac{1}{2}} + \beta_0 \quad , \tag{28}$$

where $\beta_0 = \ell n\ [a^2/8\pi ST]$ and $\beta_1 = x(4\pi\frac{S}{T})^{\frac{1}{2}}$. From this equation, notice that β_1 has dimensions of $\sqrt{\text{time}}$.

With Eq. (28) and the spectral estimates $\hat{\phi}_{hh}(f,x)$ and $\hat{\phi}_{QQ}(f)$, linear regression can be performed and the adequacy of the model determined. The coefficients β_1 and β_0 from regression are used to estimate the parameters S/T and a. The coefficient β_1 is used to estimate S/T,

$$S/T = (\beta_1/x)^2/(4\pi) \tag{29}$$

and β_0 is used to estimate a

$$a^2 = 8\pi ST \quad \exp\ \{\beta_0\} \quad . \tag{30}$$

It is important to establish confidence intervals on the mean of the spectral relation as well as on the parameters S/T and a. This will indicate the applicability of the model. The 95% confidence interval on the mean of Eq. (28) can be computed from

$$\hat{y}_i \pm t_{0.025}\ s\left\{\frac{1}{n} + \frac{(x_i - \bar{x})^2}{\sum\limits_{i=1}^{n}(x_i - \bar{x})^2}\right\}^{\frac{1}{2}} \quad , \tag{31}$$

and the 95% confidence intervals on the parameters β_0 and β_1 are given by

$$b_1 \pm \frac{t_{0.025}\, s}{\left[\sum_{i=1}^{n} (x_i - \bar{x})^2\right]^{\frac{1}{2}}} ,$$

$$b_0 \pm \frac{t_{0.025}\, s \left(\sum_{i=1}^{n} x_i^2\right)^{\frac{1}{2}}}{\left(n \sum_{i=1}^{n} (x_i - \bar{x})^2\right)^{\frac{1}{2}}} \qquad (32)$$

where

b_1, b_0 = estimates for β_1, β_0

$\hat{y}_i$ = predicted y for a given x

$t_{0.025}$ = t distribution at the 95% confidence level

n = number of data points

$\bar{x}$ = mean of independent variable $(\bar{f})^{\frac{1}{2}}$

s = estimated standard deviation

The degrees of freedom of the estimate are n-2. The 95% confidence intervals on the parameters S/T and a can also be constructed since

$$\frac{S}{T} = \left(\frac{b_1}{1}\right)^2 \quad 4\pi \qquad (33)$$

and

$$a = \frac{\exp\ (b_o/2)}{|b_1|} \quad 4\sqrt{2}\ \pi\ S1 \qquad (34)$$

where S is assumed to be a constant.

The phase $\theta_{Qh}(f,x)$ may be used to estimate the parameter S/T, as well as to indicate how much one series leads or lags the other. The linear relationship between θ_{Qh} and $f^{\frac{1}{2}}$ is expressed by

$$\theta_{Qh}(f,x) = b\, f^{\frac{1}{2}} + \frac{\pi}{4} \quad . \tag{35}$$

The coefficient b is related to S/T by the following,

$$\frac{S}{T} = (b/x)^2/\pi \quad , \tag{36}$$

where the coefficient b has dimensions of $\sqrt{\text{time}}$. For a linear association between frequency and phase, the time lag t_f at each frequency f can be computed by

$$t_f = \theta_{Qh}/(2\pi f) \quad . \tag{37}$$

Analysis of Data

Water level series of four wells were used in the analysis. Three wells are located along the Rio Hondo (Nos. 8, 11, 12), and one well (No. 7) is near the Rio Peñasco (see Fig. 2). U.S.G.S. Diamond 'A' stream gauge No. 3905 was used because of its long record and location, which is relatively close to the Rio Hondo wells. Records from observation well No. 7 near the Peñasco and the U.S.G.S. Dayton gauge No. 3985 provided data in the southern drainage.

Well No. 8 (P.V.A.C.D. observation well) is located 2 to 3 miles upstream from the Diamond 'A' gauge and is approximately 1056 feet north of the easterly flowing Rio Hondo. The Hondo meanders at this location, so that the measured distance from the well to the stream is approximate.

Figures 9a and 9b display the monthly average water level (feet) and streamflow (cfs) series. Figure 9c is a graph of the dependent variable $\ell n \left[f \left(\hat{\phi}_{hh} / \hat{\phi}_{QQ} \right) \right]$ and the independent variable $f^{\frac{1}{2}}$ from Eq. (28). The regression coefficients β_0 and β_1 along with the correlation coefficient, ρ, are listed; the dashed lines indicate the 95% confidence interval for the mean (Eq. (31)).

Further details of the calculations are given in Appendix B.

The correlation coefficient ρ was found to be 0.92, indicating that the model describes the stream-aquifer system at well No. 8 quite satisfactorily. Introducing the slope of the regression

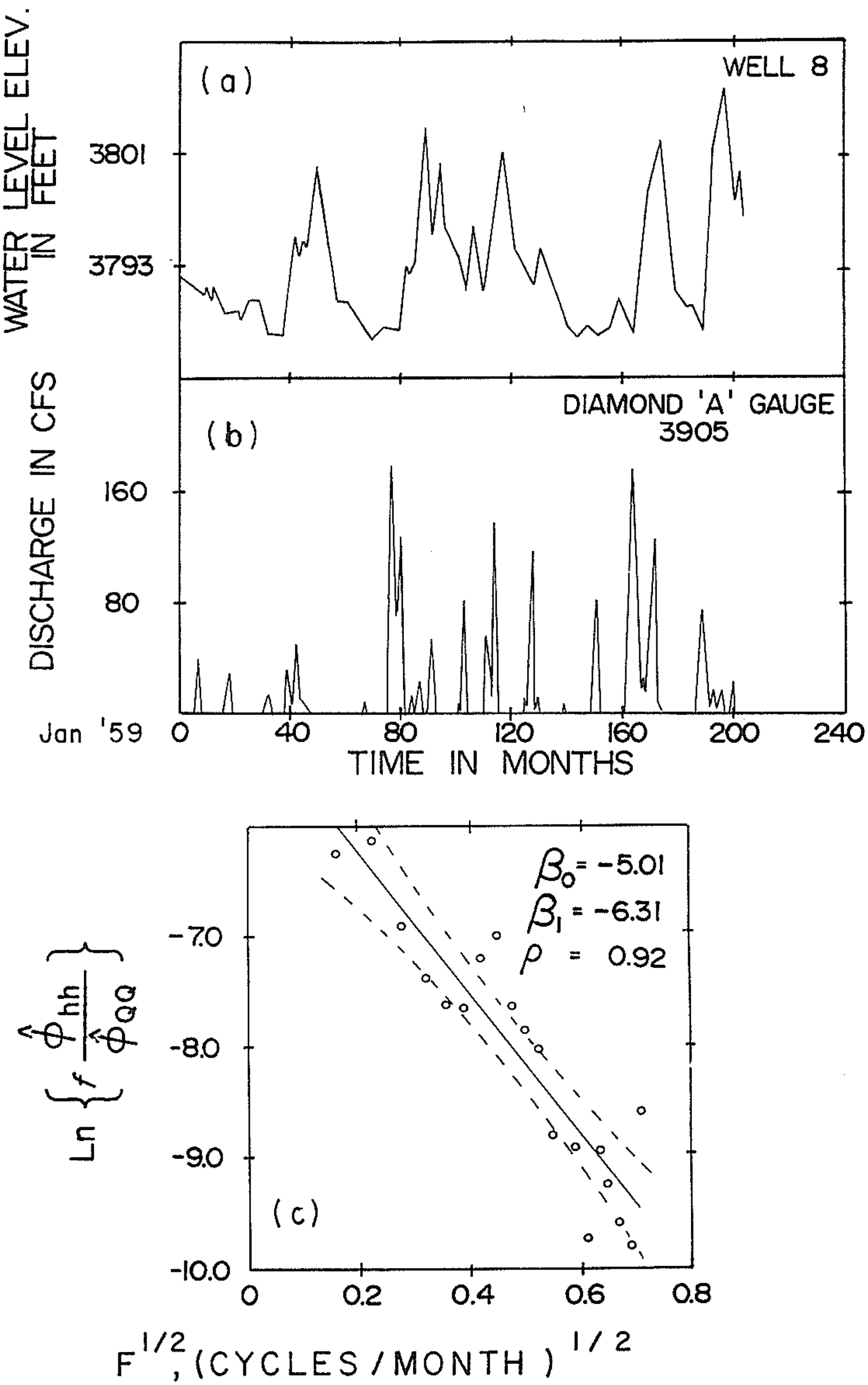

Fig. 9: Spectral analysis of well response to streamflow.
(a) Water level series at Well No. 8
(b) Streamflow at Diamond 'A' Ranch
(c) Linear form of spectral density function (Eq. (28)).
Dashed lines: 95% confidence interval.

line, $b_1 = -6.31$, into Eq. (29) the ratio S/T was found to be 8.52 x 10^{-5} day/ft^2. The 95% confidence interval on the estimate b_1 and therefore S/T (Mood and Graybill, 1963) is given by

$$-7.68 < b_1 < -4.94 \tag{38}$$

where b_1 has units of $\sqrt{\text{month}}$. For the usual units of T (ft^2/day), the 95% confidence interval for S/T is

$$5.22 \times 10^{-5} \leq S/T \leq 1.26 \times 10^{-4} \quad [\text{day/ft}^2] \ . \tag{39}$$

The parameter $\underline{a}$, or the fraction of streamflow that is recharge, can be computed from Eq. (30) if either S or T is known. Assuming the effective porosity, S, to be 0.10 the recharge parameter $\underline{a}$ was found to be 24.3 $\left(\frac{1}{\text{ft}} \frac{\text{sec}}{\text{month}}\right)$. An approximate value for recharge $\underline{q}$ per foot or channel near well No. 8 can be computed from,

$$\bar{q} = a\bar{Q} \tag{40}$$

where $\bar{Q}$ is the average discharge in cfs. Using the mean discharge at Diamond 'A' (20 cfs) q was found to be 16.2 ft^3/day per foot of channel. Confidence intervals on $\underline{b_0}$ and $\underline{a}$ are given by

$$-4.31 < b_0 < -5.71 \tag{41}$$

and

$$17.12 < a < 34.48 \quad \left[\frac{1}{\text{ft}} \frac{\text{sec}}{\text{month}}\right] \ . \tag{42}$$

Two other wells along the Hondo (No. 11 and No. 12) were used in the analysis. These wells were measured bi-monthly during the period 1956-62 by the U. S. Geological Survey. Since their location is 15 to 17 miles upstream from the Diamond 'A' gauge, some error is expected.

Well No. 11 (R. O. Anderson well) is located approximately 1980 feet south of the Hondo near Picacho, New Mexico. Figures 10a and 10b are the water level and streamflow series, and Figure 10c is the regression from Eq. (28). The much lower correlation coefficient of 0.51 indicates that the model does not completely describe the process. Since this well is some distance (~2000 ft) from the stream, recharge from excess irrigation and precipitation are probably affecting water levels.

Well No. 12 (also an R. O. Anderson well) is 515 feet north of the Hondo near Picacho. The original series and regression results are given in Figure 11. A correlation coefficient of 0.89 indicates good agreement with the proposed recharge mechanism of the model.

A tabulation of Rio Hondo wells, their location, and estimated parameters are given in Table III. It has been mentioned that prior knowledge about effective porosity, S, or transmissivity, T, is required to determine the parameter a. Since no hydrogeologic data are available in this region, a cannot be computed with certainty. To arrive at an estimate of a, the effective porosity S was assumed to be 0.10 for all cases. The average effective porosity of the Yeso and Glorieta aquifers probably does not exceed 0.20, and in general, it is likely to be much less.

The amount of recharge q at well No. 12 is estimated to be

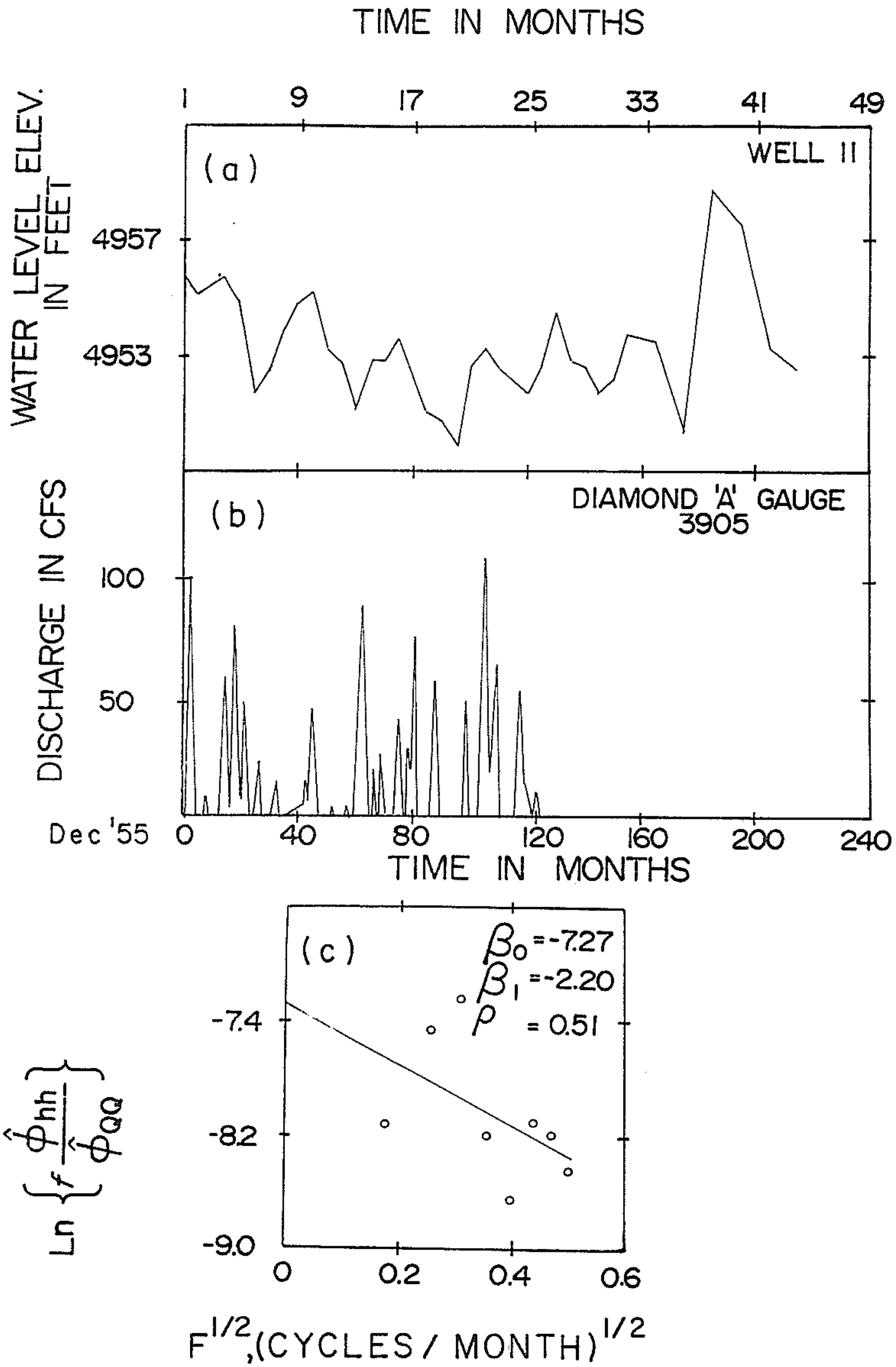

Fig. 10: Spectral analysis of well response to streamflow.
(a) Water level series at Well No. 11
(b) Streamflow at Diamond 'A' Ranch
(c) Linear form of spectral density function (Eq. (28)).
Note different time scales in (a) and (b).

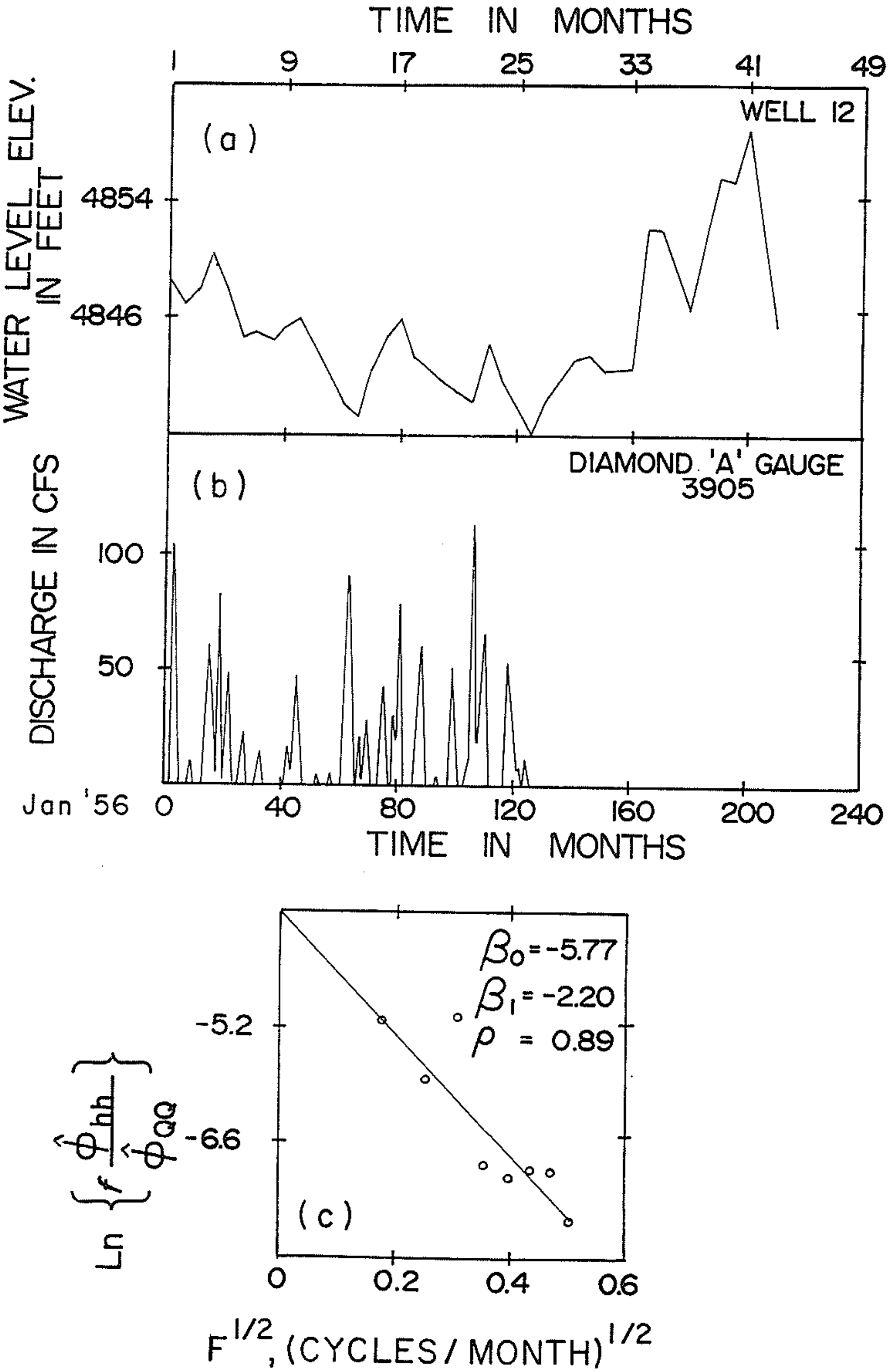

Fig. 11: Spectral analysis of well response to streamflow.
(a) Water level series at Well No. 12
(b) Streamflow at Diamond 'A' Ranch
(c) Linear form of spectral density function (Eq. (28))
Note different time scales in (a) and (b).

Table III. Model Parameters for Wells Used in this Study for Estimating Recharge Due to Channel Leakage by Rio Hondo.

Well No.	Well Location	Distance from the Rio Hondo x(feet)	$\frac{S}{T}\left(\frac{day}{ft^2}\right)$	$a\left(\frac{1}{ft}\ \frac{sec}{month}\right)$	$q(ft^3/month\text{-}ft)$
# 8	11S.21E.18.333	1056	8.52×10^{-5}	24.3	486
#12	11S.18E.24.341	515	4.35×10^{-5}	23.2	466
#11	11S.18E.16.444	1980	2.95×10^{-6}	42.2	844
Mean parameters:			4.38×10^{-5}(1)		599(2)

(1) Assuming $S = 0.10$: $T = 2.28 \times 10^3\ ft^2/day$

(2) The direct correlation between gauges (Fig. 8) gave 220 $ft^3/month\text{-}ft$

15.5 (ft^3/day - ft), indicating a similarity with results from well No. 8. However, recharge at well No. 11 is computed to be much higher, 28.1 (ft^3/day - ft). The parameters calculated for No. 11 are more likely to be in error because of the low correlation coefficient in that case. It is also important to note that recharge $\underline{q}$ at a particular location depends on the stream discharge at that location, and estimates at any one location may not be representative of the entire channel length.

Using the mean recharge computed at wells 8, 11, and 12 with an approximate channel length of 20 miles (Tinnie to Diamond 'A' Ranch), an approximate estimate of total recharge is 17,425 acre-ft/yr. Bean (1949, p. 24) estimated 19,400 acre-ft/yr on the basis of the 1944 streamflow data.

Observation well No. 7 is located about 13 miles east of Elk, New Mexico. The well is positioned 500 feet north of the Rio Peñasco channel. The only long-record stream gauge on the river is ~36 miles downstream at Dayton, New Mexico (No. 3985). Discharge at Dayton is observed only during the summer rainfall season or for large rainfall events (Appendix A). Since a good deal of the river flow leaks to the groundwater reservoir between well No. 7 and the Dayton gauge, estimates of aquifer parameters and recharge were not made. However, Figure 12c indicates that streambed leakage is a significant source of groundwater recharge in the Peñasco system also.

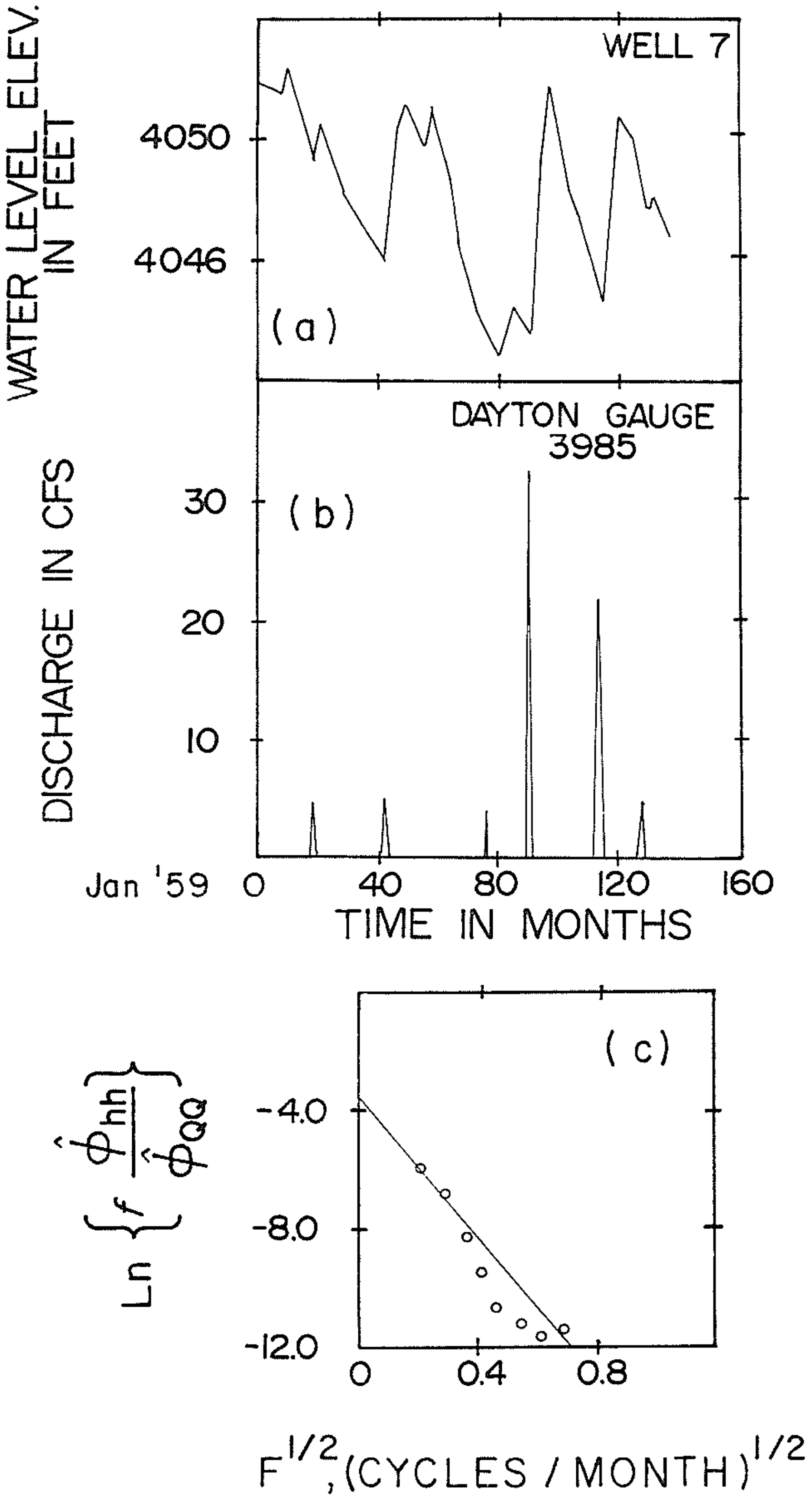

Fig. 12: Spectral analysis of well response to streamflow.
(a) Water level series at Well No. 7
(b) Streamflow at Dayton
(c) Linear form of spectral density function (Eq. (28)).

It has been shown that the phase distribution with frequency for water level and streamflow series can be used to estimate S/T from Eqs. (35) and (36). Figure 13 is a graph of the phase estimate $\hat{\theta}_{Qh}(f,x)$ versus $f^{\frac{1}{2}}$ (Table IV), computed from the cross-spectrum of water levels at well No. 8 and discharge at Diamond 'A'. The slope $b_1 = 0.52$ of the fitted line is substituted into Eq. (36) with a resulting S/T ratio of 9.15×10^{-5} day/ft^2. This result compares favorably with the previous result at well No. 8 (Table III), and thus demonstrates a useful application of the cross-spectrum and phase analysis to parameter estimation. The intercept value of 56.5° is reasonably close to the theoretical value (Eq. (35)) of $\pi/4$ (or 45°).

Equation (37) may be used as an indication of time lag between the frequency components of the water level and streamflow series. It was found that the streamflow at Diamond 'A' leads the water level at well No. 8 by 0 to 6 months for most of the indicated frequencies. For further details, the reader is referred to Appendix B.

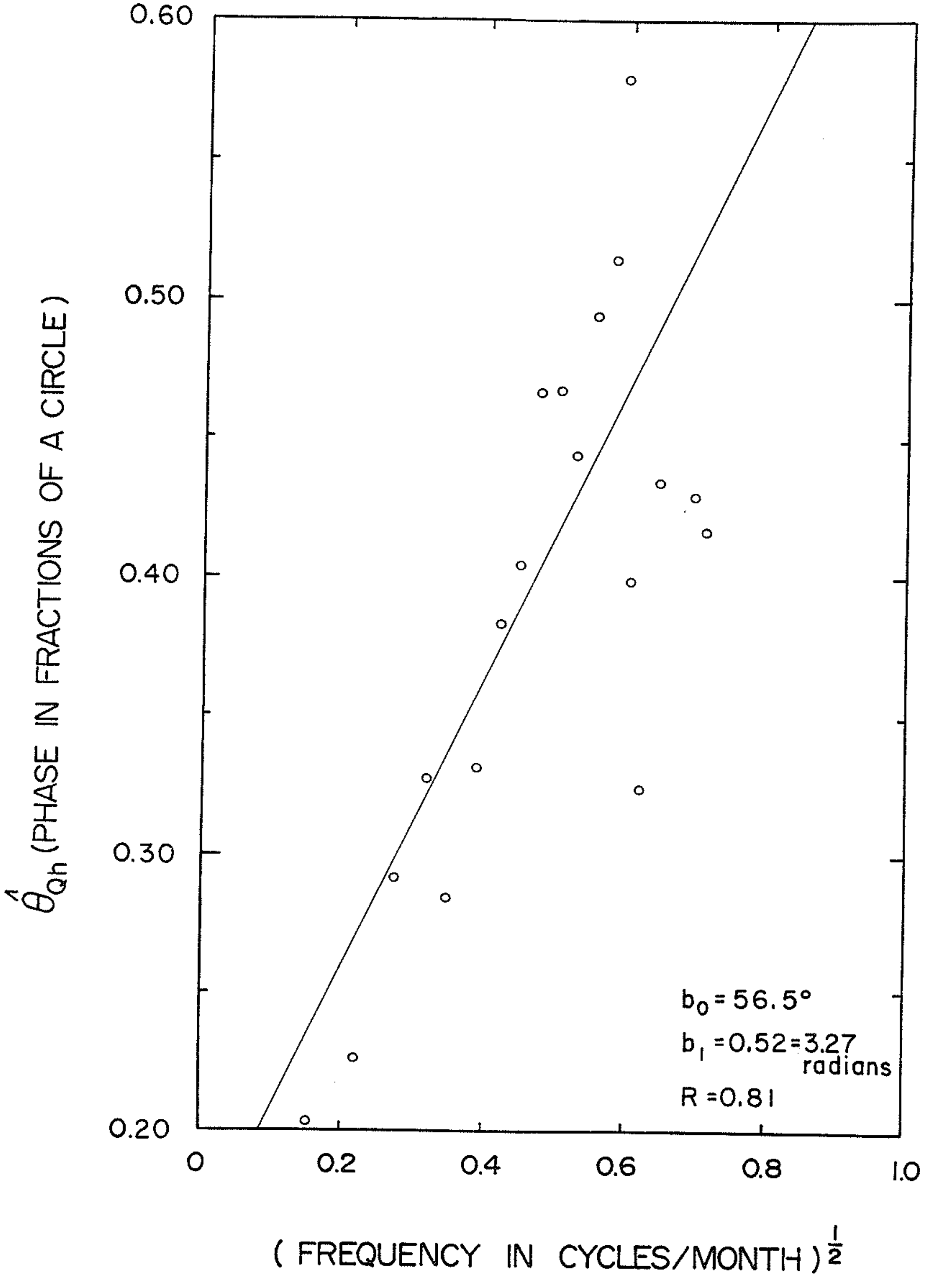

Fig. 13: The phase in fractions of a circle plotted against square root of frequency. R = correlation coefficient. Data in Table IV.

Table IV. Phase Relations Used in Spectral Computations.

Frequency (f) (cycles/month)	Phase in Fractions of a Circle (360°)	$\sqrt{f}$
0.0	.1883	0.0
.025	.2020	.158
.050	.2268	.224
.075	.2913	.274
.100	.3269	.316
.125	.2848	.354
.150	.3305	.387
.175	.3840	.418
.200	.4063	.447
.225	.4671	.474
.250	.4677	.500
.275	.4437	.524
.300	.4955	.548
.325	.5153	.570
.350	.5804	.592
.375	.3985	.612
.400	.3248	.632
.425	.4360	.652
.450	.6099	.670
.475	.4298	.689
.500	.4175	.707

Section 4

IMPORTANCE OF THE YESO AND GLORIETA AQUIFERS

Estimated Underflow to the San Andres Aquifer

In order to estimate the contribution of groundwater from the Yeso and Glorieta to the Principal Aquifer (the San Andres), it is necessary to make some restrictive assumptions. It is an unusual case where an individual aquifer can accurately be regarded as isotropic and homogeneous. Furthermore the sparsity of hydrogeologic data such as hydraulic conductivities, porosities, aquifer thicknesses and water level measurements creates a large uncertainty in this type of hydrologic estimation.

Table V is a listing of wells used in this report, giving their location, elevation, depth to water and aquifer thickness. On the basis of 8 wells located in a north-south line along the eastern boundary of the study area, an average aquifer thickness was found to be 82 feet. The gradient of the water table in this region is about 70 feet/mile, and the width of the aquifer was assumed to be 100 miles. Figure 14 is a schematic representation of the proposed underflow to the San Andres formation. Using Darcy's equation the approximate discharge from the western aquifers can be computed:

$$Q = T\,B\,J \approx 133{,}000 \text{ ac-ft/year}$$

wherein

$$T = K\bar{h} = 2.28 \times 10^3 \text{ ft}^2\text{/day} \qquad \text{(see Table III);}$$

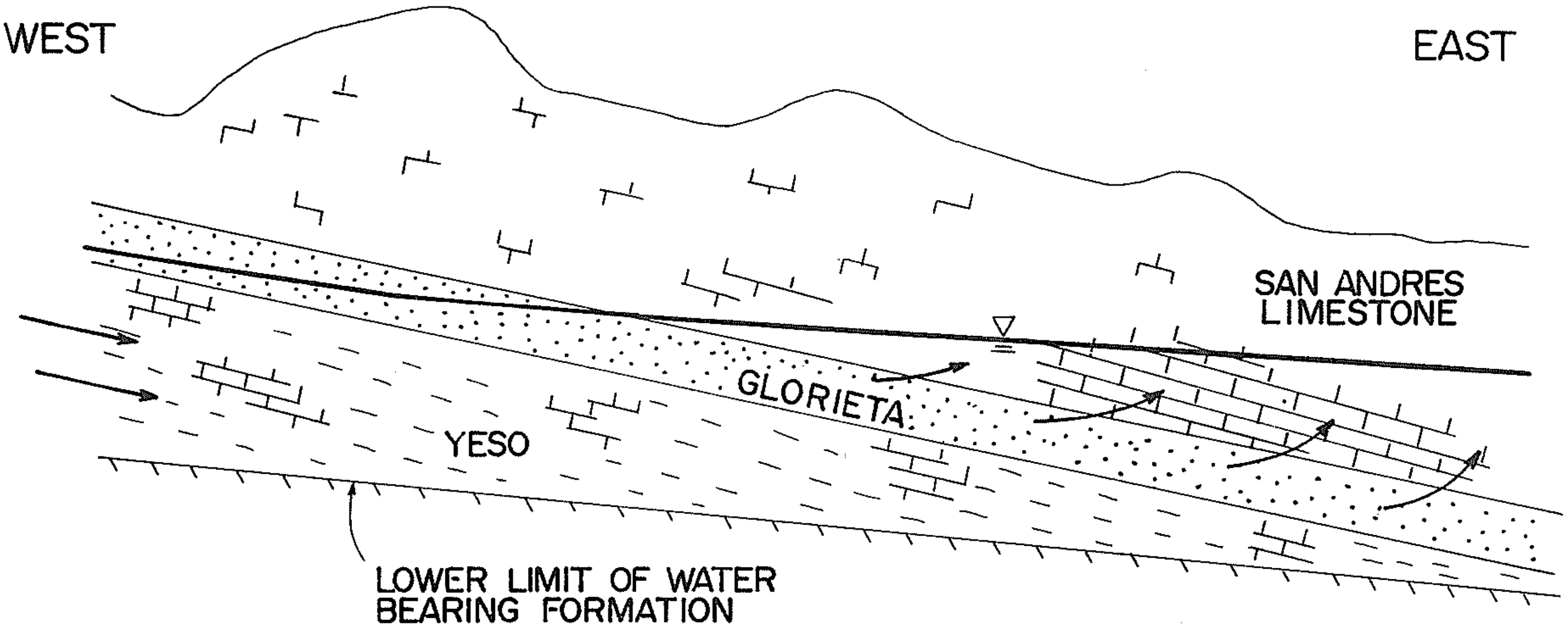

Fig. 14: Schematic East-West cross section showing underflow from Glorieta and Yeso to San Andres aquifer.

Table V. Well Listing With Characteristic Parameters.

Well #	Location	Surface Elevation (ft)	Depth to Water (ft)	Approximate Aquifer Thickness (ft)
1	7S.20E.16.333	4,694.	450 (10-26-55)	60*
2	10S.20E.16.444	4,504	437 (1-24-56)	65*
3	10S.21E.16.222	4,190	600 (3-18-56)	50*
4	13S.20E.13.222	4,524.2	263 (12- 8-55)	92*
5	16S.20E.18.333	4,488.7	600 (7-31-56)	111*
6	19S.20E.16.111	4,591	1,025 (12-24-56)	--
7	17S.20E.18.434	4,512.1	680 (2-16-57)	121*
8	11S.21E.18.333	4,283.1	410 (3-15-56)	60*
9	4S.21E.33.111	4,408.4	620 (6-18-57)	100*
11	11S.18E.16.444	5,010	60 (1-25-56)	--
12	11S.18E.24.341	4,900	51 (1-25-56)	--
			Average Aquifer Thickness:	82.4 ft

*Based on logs from Crawford and Borton (1958).

$B = 100$ miles

$J = dh/dx = 0.01326$ ft/ft $= 70$ ft/mile .

More reliable estimates can be forthcoming only when more detailed hydrogeologic data are available. These figures, along with generally low tritium values found in the Principal Intake Area, indicate the importance of possible large-scale underflow into the San Andres aquifer from the west.

SUMMARY AND CONCLUSIONS

The water level response of long-record observation wells indicates two mechanisms of recharge in the study area. Water levels with long-term trends are associated with recharge from regional precipitation. Several consecutive years of above average rainfall are necessary to significantly increase storage. A fluctuating, cyclic response is associated with channel leakage from major streams in the study area. This recharge mechanism was analyzed using a stochastic stream-aquifer model applied to the Rio Hondo and Rio Peñasco. As a result of the model, estimates of channel leakage and aquifer parameters could be inferred for three locations in the Rio Hondo drainage. The location of the Rio Peñasco stream gauge was too far downstream from observation well No. 7 to get reliable estimates of S/T and $\underline{a}$, but the model results indicate recharge from channel leakage is occurring in the Peñasco drainage also.

The two types of water level response are associated with characteristic tritium levels. High tritium levels in wells near streams verify a fast recharge component indicated by the model. Low tritium levels are generally found in wells not located near streams or large arroyos in the study area. These low levels of tritium are also found through most of the Principal Intake Area, and would appear to indicate longer residence times of groundwater than previously suggested (Rabinowitz and Gross, 1972). Although more study is required, it is likely that precipitation on the region outside the Principal Intake Area supplies significant recharge to the basin.

RECOMMENDATIONS

The importance of basic data to the management of a large basin is well known. In order to better understand the groundwater conditions of the western region of the Roswell basin, more detailed hydrogeologic data are necessary. An inventory of wells and construction of a detailed water table map of the western region would be an important first step. Compilation of all available lithologic logs could be used to delineate aquifer boundaries, determine thicknesses and better describe the geology. The aquifer parameters of porosity and permeability, and their spatial distribution, need to be better defined by pumping tests or other means. Perched groundwater systems in suitably definable locations could be useful in determining the rainfall/recharge relationship from a physical standpoint. The continuation of tritium sampling, as well as general chemistry, should lead to more information about the space-time distribution of recharge. It is likely that the western aquifers are significant to the water resources of the entire Roswell groundwater basin.

Note on modeling of the basin

When more detailed hydrologic and geologic data are available for the study region, an assessment of the water resources of the entire basin in the form of a model may be possible. The numerical models developed, respectively, by the U.S.G.S. (Trescott et al., 1976) and by Prickett and Lonnquist (1971), could be useful for predicting water levels in response to pumping, and for the general management of the groundwater basin. A transport model incorporating tritium could be used with the aquifer model to further characterize the hydrology of the basin.

REFERENCES

Bean, R. T. (1949): Geology of the Roswell Artesian Basin, New Mexico, and its relation to the Hondo Reservoir. Technical Report No. 9. State of New Mexico, State Engineer Office. Santa Fe, NM, 1951. (36 pp.)

Cooper, H. H., and Rorabaugh, M. I. (1963): Ground-water movements and bank storage due to flood stages in surface streams. U. S. Geological Survey Water Supply Paper 1536-J. (pp. 343-366)

Crawford, R., and Borton, R. L. (1958): Logs of, and Water Levels in, Observation Wells in Recharge Area of Roswell Artesian Basin, in: H. O. Reeder and others: Ground-Water Levels in New Mexico, 1957. Technical Report 22, pp. 259-306. N.M. State Engineer, Santa Fe, NM (306 pp.)

Dixon, W. J., editor (1976): BMD Biomedical Computer Programs. (Health Sciences Computing Facility. Department of Biomathematics. School of Medicine. University of California, Los Angeles). University of California Press, Berkeley, CA. (773 pp.)

Fiedler, A. G., and Nye, S. S. (1933): Geology and ground-water resources of the Roswell artesian basin, New Mexico. U. S. Geological Survey Water Supply Paper 639. (372 pp.)

Gelhar, L. W. (1974): Stochastic analysis of phreatic aquifers. Water Resources Research, Vol. 10, pp. 539-545.

Gross, G. W., Hoy, R. N., Duffy, C. J. (1976): Application of Environmental Tritium in the Measurement of Recharge and Aquifer Parameters in a Semi-Arid Limestone Terrain. Report No. 080. New Mexico Water Resources Research Institute, New Mexico State University. Las Cruces, NM (212 pp.).

Hall, F. R., and Moench, A. F. (1972): Application of the convolution equation to stream-aquifer relationships. Water Resources Research, Vol. 8, pp. 487-493.

Hantush, M. S. (1957): Preliminary Quantitative Study of the Roswell Ground-Water Reservoir, New Mexico. New Mexico Institute of Mining and Technology Research and Development Division. Socorro, NM (118 pp.).

Havenor, K. C. (1968): Structure, Stratigraphy, and Hydrogeology of the Northern Roswell Artesian Basin, Chaves County, New Mexico. Circular 93. State Bureau of Mines and Mineral Resources. New Mexico Institute of Mining and Technology. Socorro, NM. (30 pp.)

Jacob, C. E. (1943): Correlation of Ground-Water Levels and Precipitation on Long Island, New York. Transactions, American Geophysical Union. Vol. 24, pp. 564-573.

Jacobs, D. G. (1968): Sources of Tritium and its Behavior Upon Release to the Environment. U. S. Atomic Energy Commission/ Division of Technical Information, (90 pp.). Available from Clearinghouse for Federal Scientific and Technical Information

National Bureau of Standards, U. S. Department of Commerce Springfield, Virginia 22151.

Jenkins, G. M., Watts, D. G. (1968): Spectral Analysis and its Applications. Holden Day (525 pp.).

Kelley, V. C. (1971): Geology of the Pecos Country, Southeastern New Mexico. Memoir 24. State Bureau of Mines and Mineral Resources. New Mexico Institute of Mining and Technology. Campus Station, Socorro, NM (75 pp.).

Kinney, E. E., Nations, J. D., Oliver, B. J., Wagner, P. G., Siwula, Th. A., and Renner, R. E. (1968): The Roswell Artesian Basin. The Roswell Geological Society, Roswell, NM (32 pp.).

Lumley, J. L., and Panofsky, H. A. (1964): The Structure of Atmospheric Turbulence. John Wiley and Sons, NY (239 pp.).

Mood, A. M., and Graybill, F. A. (1963): Introduction to the Theory of Statistics, p. 259. McGraw Hill Book Company, NY. (443 pp.).

Motts, W. S., and Cushman, R. L. (1964): An appraisal of the possibilities of artificial recharge to ground water supplies in part of the Roswell basin, New Mexico. U. S. Geological Survey Water Supply Paper 1785. (85 pp.)

Mourant, W. A. (1963): Water Resources and Geology of the Rio Hondo Drainage Basin. Technical Report 28. New Mexico State Engineer, Santa Fe, NM (85 pp.).

National Oceanic and Atmospheric Administration (U. S. Dept. of Commerce): Local Climatological Data. Environmental Data

Service. National Climatic Center. Federal Building. Asheville, NC 28801.

Prickett, T. A., and Lonnquist, C. G. (1971): Selected Digital Computer Techniques for Groundwater Resources Evaluation. Bull. 55. Illinois State Water Survey, Urbana, IL (62 pp.).

Rabinowitz, D. D., and Gross, G. W. (1972): Environmental Tritium as a Hydrometeorologic Tool in the Roswell Basin, New Mexico. Report No. 016. New Mexico Water Resources Research Institute. New Mexico State University. Las Cruces, NM (268 pp.).

Rabinowitz, D. D., Gross, G. W., and Holmes, C. R. (1977a, b, c): Environmental tritium as a hydrometeorologic tool in the Roswell basin, NM.

I. Tritium input function and precipitation/recharge relation.

II. Tritium patterns in ground water

III. Hydrologic parameters.

Journal of Hydrology. Vol. 32, pp. 3-46.

Renick, B. C. (1926): Geology and Ground-Water Resources of the Drainage Basin of the Rio Peñasco Above Hope, New Mexico. 7th Bienn. Report. New Mexico State Engineer, pp. 103-138.

Saleem, Z. A., and Jacob, C. E. (1971): Dynamic Programming Model and Quantitative Analysis, Roswell Basin, New Mexico. Report No. 10. N. M. Water Resources Research Institute, New Mexico State University, Las Cruces, NM (180 pp.).

Theis, V. C. (1951): Effect on Artesian Aquifer of Storage of Flood Water in Hondo Reservoir. Technical Report 9. New Mexico State Engineer. Santa Fe, NM (36 pp.).

Trescott, P. C., Pinder, G. F., Larson, S. P. (1976): Finite Difference Model for Aquifer Simulation in Two Dimensions with Results of Numerical Experiments. Techniques of Water Resources Investigations, Book 7, Chap. C1. U. S. Geological Survey. (116 pp.).

United States Geological Survey (U. S. Dept. of the Interior): Water Resource Data for New Mexico. 1. Surface Water Records. (Copies may be obtained from: District Chief, Water Resources Division, U. S. Geological Survey, P. O. Box 4369, Albuquerque, NM 87106).

Venetis, C. (1971): Estimating infiltration and/or the parameters of unconfined aquifers from ground water level observations. Journal of Hydrology. Vol. 12, pp. 161-169.

APPENDIX A

STREAM DISCHARGE AND WELL LEVELS

A.I. Monthly Mean Discharge at Picacho (No. 3901), cfs.

Month	1957	1958	1959	1960	1961	1962
Jan	9.65	17.4	14.2	14.0	12.8	7.61
Feb	7.5	14.0	14.0	10.4	14.0	26.3
Mar	6.81	52.1	7.94	8.73	13.3	12.1
Apr	7.32	159.	6.72	9.71	5.11	82.1
May	12.8	116.	5.04	8.09	0	34.4
Jun	5.13	6.29	13.2	36.7	1.60	3.5
Jul	40.8	10.8	9.83	22.0	6.41	
Aug	83.0	21.3	58.2	3.26	14.6	
Sep	32.1	60.3	9.79	6.54	25.4	
Oct	27.8	49.1	4.82	3.78	.83	
Nov	24.7	29.1	5.69	4.97	5.93	
Dec	21.7	19.5	11.3	9.04	5.77	

A.II. Monthly Mean Discharge at Diamond 'A' Ranch (No. 3905), cfs.

Month	1951	1952	1953	1954	1955	1956	1957	1958	1959	1960
Jan	3.8	0	.1	0	.1	0	.4	4.1	5.3	0
Feb	1.6	.1	0	0	0	0	0	1.5	0	0
Mar	0	0	.3	0	0	.1	0	30.5	0	0
Apr	0	1.9	0	0	1.0	0	.1	138.	0	0
May	0	1.9	2.2	33.7	.7	19.7	14.2	101.	0	0
Jun	0	0	19.8	4.8	0	.1	1.4	.5	.5	26.2
Jul	.1	61.7	42.3	7.4	163.	6.0	46.3	1.0	4.3	31.3
Aug	18.8	26.0	17.7	44.1	42.6	13.3	75.7	9.6	41.4	0
Sep	0	1.0	.1	26.0	35.3	0	11.2	47.0	1.4	.2
Oct	0	0	0	142.0	23.7	0	22.7	52.0	0	0
Nov	0	0	1.8	0	.1	.03	19.5	24.7	0	0
Dec	.9	0	2.0	0	.2	0	15.8	15.7	0	.9

Continued

A.II. Continued

Month	1961	1962	1963	1964	1965	1966	1967	1968	1969	1970
Jan	.16	0	2.10	0	0	13.8	.17	0	0	2.57
Feb	0	5.71	3.29	0	0	0	.001	0	0	0
Mar	0	0	.16	0	0	16.0	.007	1.44	.024	0
Apr	0	31.6	0	0	0	26.7	0	57.7	0	0
May	0	7.87	.097	0	3.97	2.58	0	41.7	.029	0
Jun	1.37	1.77	4.97	5.3	182.0	0	7.81	.003	9.73	.14
Jul	4.35	51.5	.74	.71	109.	1.34	2.63	140.	5.59	.48
Aug	5.68	42.0	0	9.10	71.7	54.9	83.7	17.9	4.65	6.65
Sep	14.5	11.4	10.2	.47	129.	32.5	13.7	8.13	118.	3.10
Oct	0	9.42	0	1.94	9.58	0	0	0	5.17	0
Nov	0	3.43	0	3.50	0	.022	0	0	13.2	0
Dec	0	5.26	0	.065	.228	0	0	0	.77	0

Continued

A.II. Continued.

Month	1971	1972	1973	1974	1975	1976
Jan	0	0	24.7	0	6.89	0
Feb	.023	0	11.9	0	18.4	.01
Mar	0	0	28.6	0	4.43	.04
Apr	0	0	76.6	0	10.70	.02
May	0	0	127.	0	17.5	8.83
Jun	0	1.23	8.23	0	0	1.59
Jul	17.2	1.85	8.15	.14	0	2.83
Aug	84.4	24.3	0	.16	1.14	
Sep	.058	177.	0	31.3	24.3	
Oct	5.10	50.9	0	79.2	0	
Nov	.97	45.3	0	57.5	0	
Dec	0	18.6	0	9.68	0	

A.III. Monthly Mean Discharge at Dayton (No. 3985), cfs.

Month	1959	1960	1961	1962	1963	1964	1965	1966	1967	1968	1969	1970
Jan	0	0	0	0	0	0	0	0	0	0	0	0
Feb	0	0	0	0	0	0	0	0	0	0	0	0
Mar	0	0	0	0	0	0	0	0	0	0	0	0
Apr	0	0	0	.17	0	0	0	0	0	0	0	0
May	0	0	0	0	0	0	41.0	0	0	0	0	.54
Jun	0	0	9.71	19.4	6.1	9.1	.2	0	0	0	0	1.79
Jul	0	48.1	0	52.4	0	3.2	1.7	0	0	221	0	0
Aug	0	2.5	0	37.6	1.0	0	0	328	7.42	0	10.5	.45
Sep	0	0	0	0	0	3.5	0	0	0	0	48.7	0
Oct	0	0	0	0	0	0	0	0	0	0	0	0
Nov	0	0	0	0	0	0	0	0	0	0	0	0
Dec	0	0	0	0	0	0	0	0	0	0	0	0

A.IV. Observation Well No. 1, Monthly Average Water Levels, Feet Below Well Collar.

Month	1961	1962	1963	1964	1965	1966	1967	1968
Jan	451.75	451.97	452.35	452.70	453.23	454.32	455.38	456.49
Feb	.74	452.00	.34	.74	.38	.38	.49	.60
Mar	.78	451.96	.44	.85	.45	.54	.55	.67
Apr	.81	452.02	.35	.68	.50	.61	.60	.76
May	.81	.01	.35	.51	.62	.74	.72	.82
Jun	.81	.08	.36	.51	.73	.78	.83	.94
Jul	.85	.09	.41	.63	.80	.89	.89	.08
Aug	.89	.15	.46	.92	.92	455.07	456.06	.40*
Sep	.88	.17	.47	.75	.91	.17	.21	.46*
Oct	.88	.19	.37	.93	.65	.22	.23	.51*
Nov	.90	.28	.58	453.02	.70	.31	.31	.34*
Dec	.94	.34	.55	.12	454.22	.19	.38	.41*

A.IV. Continued.

Month	1969	1970	1971	1972	1973	1974	1975
Jan	457.51*	454.34†	454.70	459.14	459.10	459.48	460.38
Feb	.58*	.35	.74	.16	.11	.50	.34
Mar	.58*	.35	.78	.16	.14	.52	.34
Apr	.59*	.42	.83	.18	.17	.36	.40
May	.66*	.45	.85	.21	.21	.39	.44
Jun	457.57	.48	455.13†	.21	.19	.50	.48
Jul	.57	.43	459.23†	.22	.16	.51	.47
Aug	.57	.44	.25	.18	.17	.56	461.10†
Sep	.15	.47	.25	.19	.19	.66	
Oct	455.56	.62	.52†	.03	.25	.68	
Nov	454.01	.67	.49	458.96	.32	.62	
Dec	.12	.70	.36	.99	.43	459.49	

*Interpolated

†Measured

A.V. Observation Well No. 2, Monthly Average Water Levels, Feet Below Well Collar.

Month	1959	1960	1961	1962	1963	1964	1965	1966	1967
Jan	422.39†	422.27	422.38	422.82	423.41	423.75	424.16	424.77	425.34
Feb	.41	.45	.38	.68	.39	.78	.21	.87	.32
Mar	.38	.52	.39	.61	.41	.83	.28	.93	.41
Apr	.42	.55	.43	.74	.47	.91	.34	.94	.44
May	.42	.59	.44	.91	.51	.94	.35	.98	.39
Jun	.44	.73	.50	.98	.57	.99	.41	.76	.60
Jul	.17†	.61	.51	423.06	.59	424.01	.45	.91	.66
Aug	.18†	.54	.56	.13	.64	.05	.50	425.11	.68
Sep	.25	.43	.61	.20	.65	.05	.53	.13	.65
Oct	.24	.37	.67	.23	.73	.06	.60	.38	.76
Nov	.54	.33	.72	.29	.74	.11	.64	.39	.93
Dec	.55	.29	.77	.35	.74	.11	.71	.36	.92

†Measured

Continued

A.V. Continued.

Month	1968	1969	1970	1971	1972	1973	1974	1975
Jan	425.92	426.16	426.43	426.78	425.89	424.79	424.13	423.34
Feb	426.00	.18	.39	.82	.80	.73	.11	.25
Mar	.06	.22	.35	.88	.68	.61	.10	.09
Apr	.14	.23	.35	.92	.62	.64	.10	422.80
May	.21	.25	.40	427.02	.64	.53	.11	.60
Jun	.29	.27	.45	.07	.64	.44	.03	.53
Jul	.24	.31	.50	.18	.74	.37	.04	
Aug	.22	.33	.55	.19	.80	.27	.02	
Sep	.36	.35	.58	426.92	.58	.23	423.95	
Oct	.35	.38	.59	.59	.38	.19	.87	
Nov	.24	.43	.66	.26	.19	.15	.84	
Dec	.22	.39	.72	.06	424.99	.12	.43	

A.VI. Observation Well No. 3, Monthly Average Water Levels, Feet Below Well Collar.

Month	1958	1959	1960	1961	1962	1963	1964	1965	1966	1967
Jan	589.10	589.89	589.11	589.70†	590.65	591.85	593.12	594.46	595.28	595.48
Feb	.14	.76	.14	.63	.62	.84	.16	.45	.32	.46
Mar	.16	.71	.15	.61	.70	.87	.27	.55	.29	.36
Apr	.21	.74	.23	.60†	.79	.98	.27	.63	.31	.32
May	.33	.87	.40	.71	.92	.87?	.45	.71	.35	.39
Jun	.59	590.00	.56	.82†	591.12	592.00	.59	.85	.40	.43
Jul	.80	.27	.70	590.04	.21	.23	.73	.96	.42	.51
Aug	.87	.30	.70	.22	.35†	.38	.87	595.03	.46	.60
Sep	590.06	.25	.69	.58†	.52	.47	.98	.10	.48	.62
Oct	.10	.34	.64	.70†	.76	592.75†	594.13	.22	.51	.68
Nov	.51	589.56†	.71	.68	.80	.84	.32	.24	.48	.64
Dec	.36	.14	.66	.50	.86	.96	.36	.29	.50	.65

†Measured

Continued

A.VI. Continued.

Month	1968	1969	1970	1971	1972	1973	1974	1975	1976
Jan	595.65	595.80*	595.79		595.34*	593.19*	591.75*	592.25	589.37
Feb	.69	.82*	.67		.31*	592.97*	.74*	.20	
Mar	.64	.80*	.56		.29*	.59*	.68*	.12	
Apr	.57	.76*	.64		.18*	.34*	.76*	.13	
May	.54*	.74*	.63		.25*	.16*	.78*	.13	
Jun	.62*	.77*	.60		.29*	591.99*	.91*	.15	
Jul	.62*	.80*	.60	595.29*	.32*	.84*	592.03*	.13	
Aug	.63*	.80*	.63	.28*	.33*	.77*	.16*	591.98	
Sep	.62*	.81*	.62	.26*	.24*	.76*	.17*	590.36	
Oct	.73*	.90*		.30*	.03*	.79*	.19*	589.95	
Nov	.83*	.96*		.31*	594.12*	.76*	.33*	590.08	
Dec	.78*	.85*		.26*	593.71*	.84*	.25*	589.82	

*Interpolated

A.VII. Observation Well No. 4, Monthly Average Water Levels, Feet Below Well Collar.

Month	1959	1960	1961	1962	1963	1964	1965	1966	1967
Jan	259.01	259.46	258.58	260.11	260.30	260.87	261.58†	261.46†	260.49
Feb	.10	.61	.68	.20	.50	.97†	.56†	.61†	.65
Mar	.08	.76	.83	.34	.68	261.05	.63	.73†	.83
Apr	.28	.94	.96†	.46	.79	.14†	.68†	.88†	.94
May	.44	260.12	259.14†	.55	261.04	.19	.73	.92	261.09
Jun	.53	.27	.28	.69†	260.95†	.25†	.82†	.85	.17
Jul	.68	.14	.40	.81	.86†	.34†	.88	.82†	.35
Aug	.69	259.52	.50†	.59	.70†	.36†	.84†	.82†	.49
Sep	.56	.94	.60	.26	.60†	.44†	.60†	.35†	.62
Oct	.55	.54†	.74†	.12	.45	.49†	.29	260.78	.73
Nov	.45	.41	.87	.07†	.51†	.45	.14†	.44	.63
Dec	.28	.41	260.01	.19	.70	.46†	.20	.32	.76

†Measured

Continued

A.VII. Continued.

Month	1968	1969	1970	1971	1972	1973	1974	1975
Jan	261.86	262.45	262.58	262.92	262.32	260.10	260.76	256.93†
Feb	262.04	.61	.69†	.93	.38	.07	.84	.25
Mar	.08	.68	.67	.96	.46	.05	.85	255.92
Apr	.11	.79	.70	.93	.53	.20	.86	.72
May	.06	.90	.71	.94	.58	.35	.92	.63
Jun	.10	.97	.71	.94	.67	.42	.95	.72
Jul	261.93	263.02	.76	263.02	.75	.47	261.01	.74
Aug	.64	262.32†	.78†	264.38†	.83	.51	.05	.75
Sep	.80†	.35	.80	.07	.43	.54	260.95	.37†
Oct	262.19†	.43	.80†	263.77	261.53	.58	.42	.34
Nov	.25	.50	.84	262.24	260.73	.59	259.35	.47
Dec	.32	.50	.88	.29	.15	.64	258.02	.58

†Measured

A.VIII. Observation Well No. 7, Monthly Average Water Levels, Feet Below Well Collar.

Month	1959	1960	1961	1962	1963	1964	1965	1966
Jan	460.30	460.92	462.77	465.39	461.12	462.59†	467.77†	467.76
Feb	.44	461.19	463.17	.61	.40	.90	468.09	.93
Mar	.53	.87	.53†	.78	.64†	463.31	.38†	468.09
Apr	.55	462.12	.87	466.00	462.04†	.42†	.55	.36†
May	.38	.58	464.15	.14	.29†	.68	.80	.47†
Jun	.46	.93	.37†	465.80	.34	464.00	.93	.61
Jul	.71	.18	.53	.32†	.32	465.79†	469.10†	.37
Aug	.30	461.58	.63	463.95	.22	466.46	.18	467.32
Sep	459.70	.79	.72†	462.46	.07	.70†	468.81	464.89
Oct	.86	.90	.84	461.61	460.96	.99†	.32	462.72†
Nov	460.06	462.07	465.02	.20†	461.59	467.25†	467.88	461.08
Dec	.47	.38	.20†	.00	.79	.49	.67	460.34

†Measured

Continued

A.VIII. Continued.

Month	1967	1968	1969	1970	1971	1972	1973	1974
Jan	460.46	465.57	461.61	464.45				460.06
Feb	.98	466.05	.76					.10*
Mar	461.59	.48	.82	.98*				.20*
Apr	462.08	.95	462.01	465.25*				.70*
May	.65	467.24	.44	.42*				.86
Jun	463.21	.56	463.02					461.29
Jul	.70	.58	.60					
Aug	464.03	466.66	464.30				457.84	
Sep	.35	465.00	.43				458.58	
Oct	.63	463.30†	.18				459.24	
Nov	.79	461.45†	.04				.74	
Dec	465.27	.25	.20		464.80		.95	

†Measured

*Interpolated

A.IX. Observation Well No. 8, Monthly Average Water Levels, Feet Below Well Collar.

Month	1959	1960	1961	1962	1963	1964	1965	1966	1967
Jan	397.20	398.00*	398.60†	401.28	389.53	398.90	401.08	396.16	393.85
Feb	.60	399.05	.97	400.90	.38	399.28	400.83†	394.50	394.65
Mar	.53	.26	.84	.60	390.20	.67†	.89†	393.45	.79
Apr	.63	.85	.66	399.88	.98	.76†	.98	390.58	395.26
May	.89	400.02	.95	394.88†	393.30†	.92	.94	386.63†	.70†
Jun	398.13	399.90	399.77†	.25	396.28†	400.28†	401.17	388.95	396.48
Jul	.40	.85	400.61†	395.90†	397.63	.71	.32	392.33	397.80
Aug	.46	.52	401.24	.52	398.35	401.09	400.13	394.58	398.30
Sep	.14	.70	.05†	394.79	.96†	.28	397.93	392.85	396.06
Oct	.00	400.45	.38	395.51	399.04†	.38	396.57	388.91	393.44†
Nov	.63	399.95	.37	391.95†	398.90†	.48	397.19	391.05	394.71†
Dec	399.01	.52	.40	390.13†	.92†	.23	396.46	393.12	396.70

†Measured

*Interpolated

Continued

A.IX. Continued

Month	1968	1969	1970	1971	1972	1973	1974	1975
Jan	397.98	395.87	396.50	401.50*	400.16†	391.32*	398.76	387.90†
Feb	398.17	.50	.90†	.36	399.28†	.30	399.25	.16
Mar	.10	.88	397.80	400.88	398.72	390.28	.51	385.15
Apr	396.80	396.63	398.71	.70*	399.29	389.21	.44	383.58
May	394.10	397.01	399.39†	401.23*	400.04	388.07	.41	384.18
Jun	392.50	.32	.88	.39	.63	387.33*	.84*	385.36
Jul	390.70†	.72	400.29	.50*	401.08	389.28	400.48*	387.54
Aug	389.51†	398.15	.67†	.67†	.34	393.04	.69	390.34†
Sep	388.16	397.94	401.00	.20†	400.28	395.23*	401.14*	391.17
Oct	389.20†	395.09	.31	.05†	397.28	396.21	400.10*	389.56
Nov	392.52	.40	.52	.09	393.71†	397.98	398.29*	392.30*
Dec	395.26	.60	.35*	400.82*	391.57	398.77†	390.33†	393.20†

†Measured

*Interpolated

A.X. Observation Well No. 9, Monthly Average Water Levels, Feet Below Well Collar.

Month	1959	1960	1961	1962	1963	1964	1965	1966	1967
Jan	593.90	594.02	592.53	592.38	592.20	591.66	591.28	590.43	590.26
Feb	.96	593.64	.44	.39	.00	.55	.08	.47	.29
Mar	.91	.06	.40	.43	591.95	.65	.07	.42	.28
Apr	.98	.11	.40	.18†	.85	.62	.11	.44	.30
May	.99	.10	.46	.16	.90†	.71	.06	.43	.29
Jun	594.07	.20	.47	.26	.74	.75	590.99	.51	.37
Jul	.08	.16	.48	.23	.69	.79†	.88	.52	.40
Aug	.08	.01†	.50	.19	.69	.81	.74	.60	.40
Sep	.02	592.88	.45†	.20	.82†	.85	.63	.69	.26
Oct	.10	.71	.43	.27	.96	.84	.62	.62	.23
Nov	.11	.67	.46†	.25	.79	.79	.49	.37	.27
Dec	.05	.58	.42	.29	.70	.70	.52	.29	.28

†Measured

Continued

A.X. Continued.

Month	1968	1969	1970	1971	1972	1973	1974	1975
Jan	590.30	589.95†	589.50	590.23	589.90	590.33	590.61	590.80
Feb	.31	.86	.64	.23	.82	.35	.59	.93
Mar	.39	.78	.58	.39	.91	.50	.55	.85
Apr	.33	.71	.65		.95	.62	.52	.90
May	.33	.58	.62		.99	.55	.55	.80
Jun	.38	.40	.68	.43	590.10	.56	.57	.74
Jul	.41	.50	590.25		.16	.64	.65	.47
Aug	.27	.49	.22	589.79	.22	.66	.61	.25†
Sep	.12	.55	.22	.77	.27	.52	.47*	589.98
Oct	.00	.59	.35	.80	.27	.54	.72	590.68
Nov	588.89†	.59	.19	.88	.33	.58	.68	.72
Dec	.84	.50	.18	.95	.39	.52	.75	.78

†Measured

*Approximate Value

A.XI. Well No. 11, Bimonthly Average Water Levels, Feet Below Well Collar.

Date	Depth to Water
10-26-55	54.14
12-10-55	54.51*
1-25-56	54.88
3-20-56	54.48
5-15-56	54.28
7-24-56	55.17
9-24-56	58.30
11-28-56	57.48
1- 2-57	56.04
3-26-57	55.18
5-15-57	54.75
7-23-57	56.68
9-25-57	57.26
11-15-57	58.87
1-15-58	57.14
3-26-58	57.20
5-20-58	56.30
7-24-58	57.75
9-16-58	58.96
11-25-58	59.31
1-15-59	60.18
3-25-59	57.30
5-26-59	56.70
7-24-59	57.45
9-25-59	57.84
11-25-59	58.35
1-13-60	57.39
3-23-60	55.56
5-26-60	57.17
7-22-60	57.39
9-23-60	58.32
11-23-60	57.85

---

*Two-point average to synthesize missing data

Continued

A.XI. Continued.

Date	Depth to Water
1- 3-61	56.14
3- 4-61	56.32*
5- 3-61	56.50
7-28-61	58.10
9-28-61	59.70
11-16-61	55.47*
1- 3-62	51.23
3- 3-62	51.84*
5- 1-62	52.45
7- 8-62	54.55*
9-14-62	56.65
11- 8-62	57.05*
1- 2-63	57.45

* Two-point average to synthesize missing data

A.XII. Well No. 12, Bimonthly Average Water Levels, Feet Below Well Collar.

Date	Depth to Water
5-12-55	45.90
1-25-56	51.14
3-21-56	53.20
5-15-56	52.25
7-24-56	49.65
9-24-56	51.94
11-28-56	55.50
1- 2-57	55.07
3-26-57	55.66
5-15-57	54.66
7-23-57	54.00
9-25-57	55.48
11-25-57	57.60
1-15-58	59.76
3-26-58	60.80
5-21-58	57.40
7-24-58	55.20
9-16-58	54.08
11-25-58	56.72
1-15-59	57.43
3-25-59	58.44
5-26-59	59.00
7-24-59	59.89
9-25-59	55.67
11-25-59	58.30
1- 7-60	60.13*
3-23-60	61.95
5-26-60	59.70
7-22-60	58.36
9-23-60	56.85
11-23-60	56.47

---

*Two-point average for missing data synthesis

Continued

A.XII. Continued.

Date	Depth to Water
1- 3-61	57.69
3- 4-61	57.61*
5- 3-61	57.52
7-28-61	47.65
9-28-61	47.82
11-15-61	50.67*
1- 3-62	53.52
3- 3-62	48.86*
5- 1-62	44.20
6-25-62	44.59
9-14-62	40.90
11- 8-62	47.57*
1- 3-63	54.24

* Two-point average for missing data synthesis

APPENDIX B

SPECTRAL REPRESENTATION OF TIME SERIES AND THEIR ESTIMATORS

SPECTRAL REPRESENTATION OF TIME SERIES

In a statistical sense a time series can be considered a random or non-deterministic function which, because of its inexact nature, is necessarily described by probability laws. To describe the function statistically it is convenient to regard a particular time series as one realization of another set of functions called a stochastic process. The most important assumptions about the time series are that the associated stochastic process is stationary, and the stationary process is adequately described by the lower moments of its probability distribution, i.e., the mean, variance and covariance.

The mean can be written as

$$\bar{x} = E[x(t)] = \int_{-\infty}^{\infty} x\, p(x)\, dx \qquad \text{B.1}$$

where $p(x)$ is the probability density function.

The covariance is expressed as

$$R_{xx}(\tau) = E[x(t)\, x(t+\tau)] = \int_{-\infty}^{\infty}\int_{-\infty}^{\infty} x_1 x_2\, p(x_1,x_2)\,dx_1 dx_2 \qquad \text{B.2}\ ,$$

where x_1 and x_2 correspond to $x(t)$ and $x(t+\tau)$, respectively, and $p(x_1,x_2)$ is the joint probability density function. At $\tau = 0$ $R_{xx}(0)$ becomes the variance.

The classical Fourier representation of series or integrals does not apply to random functions since they are neither periodic nor integrable. But there does exist a random process $z(\omega)$

from which a time series x(t) can be expressed as

$$x(t) = \int_{-\infty}^{\infty} e^{i\omega t} dz(\omega) \qquad \text{B.3}$$

Equation B.3 is known as a stochastic Fourier-Stieltjes integral (Lumley and Panofsky, 1964).

The differences $dz(\omega)$ are the complex Fourier amplitudes of the process, $z(\omega)$, with frequency ω. The process $z(\omega)$ has the property of nonoverlapping increments or,

$$E[dz(\omega_1) \cdot dz^*(\omega_2)] = \begin{cases} 0, \omega_1 \neq \omega_2 \\ \phi(\omega)d\omega, \ \omega_1 = \omega_2 \end{cases} \qquad \text{B.4}$$

where the star denotes a complex quantity.

and

$$F(\omega) = \int_{-\infty}^{\omega} \phi(\omega)d\omega \quad , \qquad \text{B.5}$$

with $F(\omega)$ denoting the power spectral distribution.

The derivative of the power spectral distribution can be used to arrive at the autocovariance,

$$R_{xx}(\tau) = \int_{-\infty}^{\infty} e^{i\omega\tau} d\ F(\omega) = \int_{-\infty}^{\infty} e^{i\omega\tau}\phi(\omega)d\omega \qquad \text{B.6}$$

$\phi(\omega)$ is the spectral density function of x(t), or simply the spectrum, and is related to the autocovariance by the Fourier transform pair given in B.6 and B.7

$$\phi(\omega) = \frac{1}{2\pi} \int_{-\infty}^{\infty} e^{-i\omega\tau} R(\tau)d\tau \quad . \qquad \text{B.7}$$

A stationary random process, then, is simply described by its autocovariance, or the Fourier transform of the autocovariance, the spectrum. The spectrum shows how the variance of the process is distributed with frequency ω.

Estimators and Confidence Intervals

This subsection is devoted to the procedure of estimating the spectrum and covariance functions from observed time series. It is quite often not possible or feasible to obtain continuous hydrologic data, so discrete estimations are necessary. The sampling interval, Δt, must contain the desired information if the modeling experiment is to be successful. For example, the water level data used in this report were available at 8 hour intervals for nearly 20 years (Well No. 8). However, these finely spaced data were examined and found not to contain additional information with regard to the recharge problem. A time interval, Δt, of one month was considered adequate. By averaging the 8 hour data over each month the resulting covariance and spectral estimates were smoothed or filtered, thus improving results. The sampling interval, Δt, then, is of considerable importance, since too finely spaced data would greatly increase computation time and cost, while data too widely spaced would cause errors by actually losing information. The loss of data from too large a time interval is called aliasing.

The discrete estimation formula for the autocovariance, $\hat{R}_h$, is given by

$$\hat{R}_h(j) = \frac{1}{N-j} \sum_{i=1}^{N-j} \left\{ (h_i-\bar{h})(h_{i+j}-\bar{h}) \right\} , \qquad \text{B.8}$$

where $\underline{j}$ represents the lag, $\underline{N}$ is the sample size and $\underline{\bar{h}}$ is the mean of the variable.

By recalling the Fourier transform pair described earlier (B.6, B.7), the spectrum $\phi_h(\omega)$ can be estimated by

$$\hat{\phi}_h(\omega) = \frac{1}{2\pi}\left[\hat{R}(0) + z\sum_{j=1}^{M} \hat{R}(j)\cos(j\omega)\right], \qquad \text{B.9}$$

where hats denote estimators.

In order to obtain consistent values of $\hat{\phi}_h(\omega)$ it is necessary to smooth the spectral estimator using a set of weighting factors which is usually called a spectral window; the Hamming window is used in the BMD program.

The number of degrees of freedom for the smoothed spectral estimate is given by

$$\nu = 2.78\ N/M\ , \qquad \text{B.10}$$

where N is the length of record and M is the maximum lag (Jenkins and Watts, p. 252). Equation B.10 results from the 'window' used to smooth the spectral estimate (Hamming window). The degrees of freedom can now be used to construct confidence intervals on the spectral estimates.

The distribution of the smoothed spectral estimator is approximately chi-square, χ^2_ν , with ν degrees of freedom. The 1-α confidence interval is given by

$$\frac{\nu\hat{\phi}(\omega)}{\chi^2_\nu(1-\alpha/2)} \le \hat{\phi}(\omega) \le \frac{\nu\hat{\phi}(\omega)}{\chi^2_\nu(\alpha/2)} \qquad \text{B.11}$$

Eq. B.11 gives a confidence interval for $\hat{\phi}(\omega)$ at a particular frequency only. Rewriting B.11 in terms of natural logarithms makes the confidence interval a constant value given by

$$\mathrm{Ln}\ \hat{\phi}(\omega) + \mathrm{Ln}\ \frac{\nu}{x_\nu(1-\alpha/2)} \leq \mathrm{Ln}\ \phi(\omega) \leq \mathrm{Ln}\ \hat{\phi}(\omega)$$

$$+ \mathrm{Ln}\ \frac{\nu}{x_\nu(\alpha/2)} \quad . \qquad \text{B.12}$$

Eq. B.12 was used to establish confidence intervals on the spectral estimators given in this subsection. Table B.I. is a listing of pertinent data used.

Figures B.1 through B.4 are graphs of the spectral estimates, on the Ln scale, of water levels and stream discharges plotted against frequency (cycles/month) which were used in the stochastic model. The parameters used are given in Table B.I. Spectral estimates are given in Tables B.II through B.IV.

The solid line in each case represents the stream discharge spectrum and the dashed line indicates the water level spectrum. The streamflow spectrum for each graph is characteristic of an uncorrelated random process or white noise. On the other hand the water level spectrum illustrates the typical response of a highly damped groundwater system in that high-frequency components of the water level spectrum are attenuated. This can also be explained as a filtering of the input spectrum (streamflow) which reduces the output spectrum (head) at high frequency.

Table B.I. Well Parameters Used for Spectral Estimates.

Time Series	Length of Record (mos.)	No. of Lags	Filtering	Deg.'s of Freedom
Well No. 8	204	20	Average 8 Hr. Data	28
Diam. 'A' Gage	204	20	Monthly Mean	28
Well No. 11	45	9	None	14
Well No. 12	43	9	None	13
Well No. 7	137	13	Average 8 Hr. Data	29
Dayton Gage	137	13	Monthly Mean	29

NOTE: All spectral estimates in this report were computed with the BMD02T computer program written by the Health Sciences Computing Facility, Dept. of Biomathematics, UCLA, 1976.

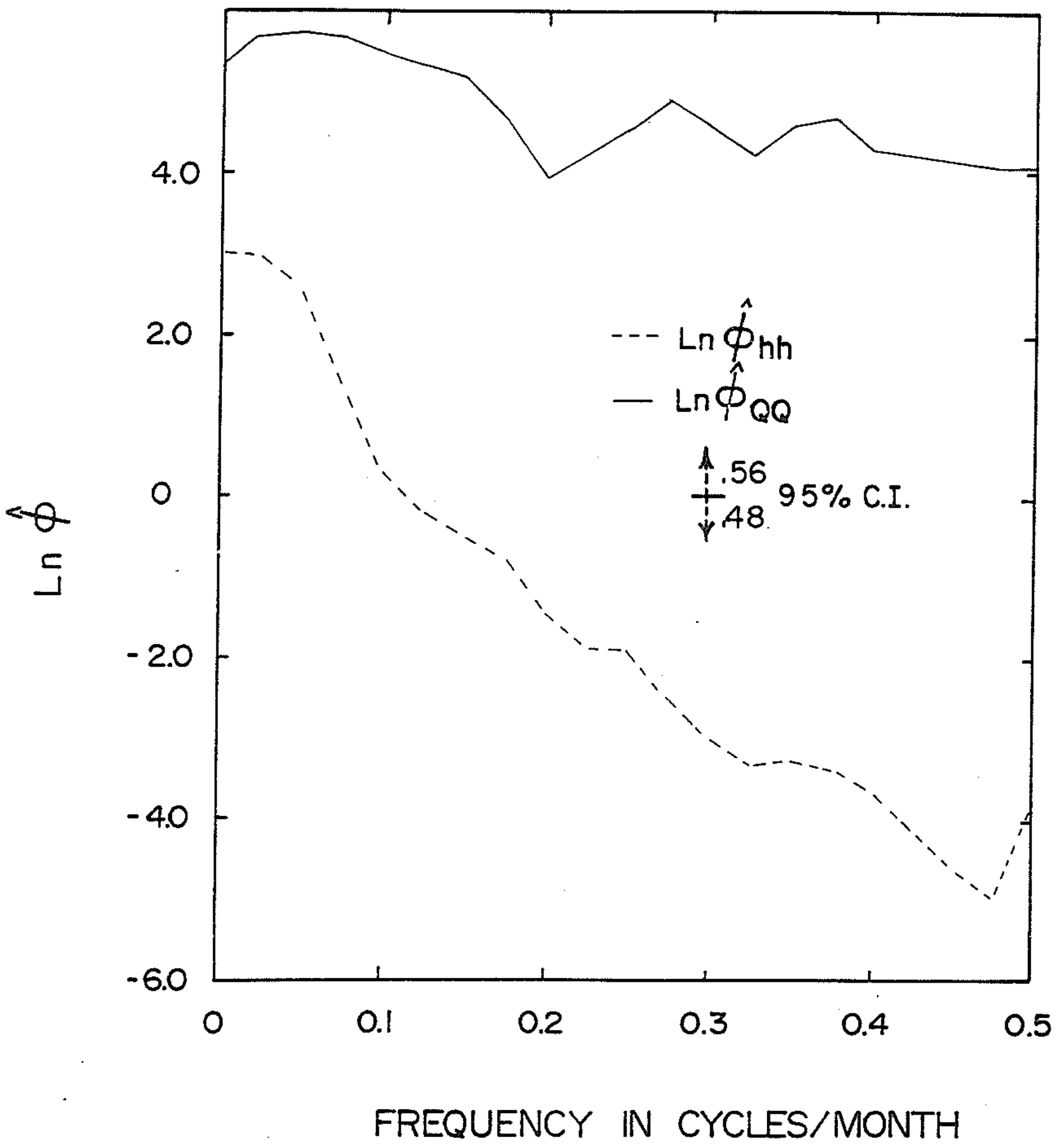

Fig. B.1 Spectral estimates of water level at Observation Well No. 8 (Ln $\hat{\phi}_{hh}$) and discharge at Diamond 'A' Ranch (Ln $\hat{\phi}_{QQ}$), versus frequency. Data listed in Table B.II.

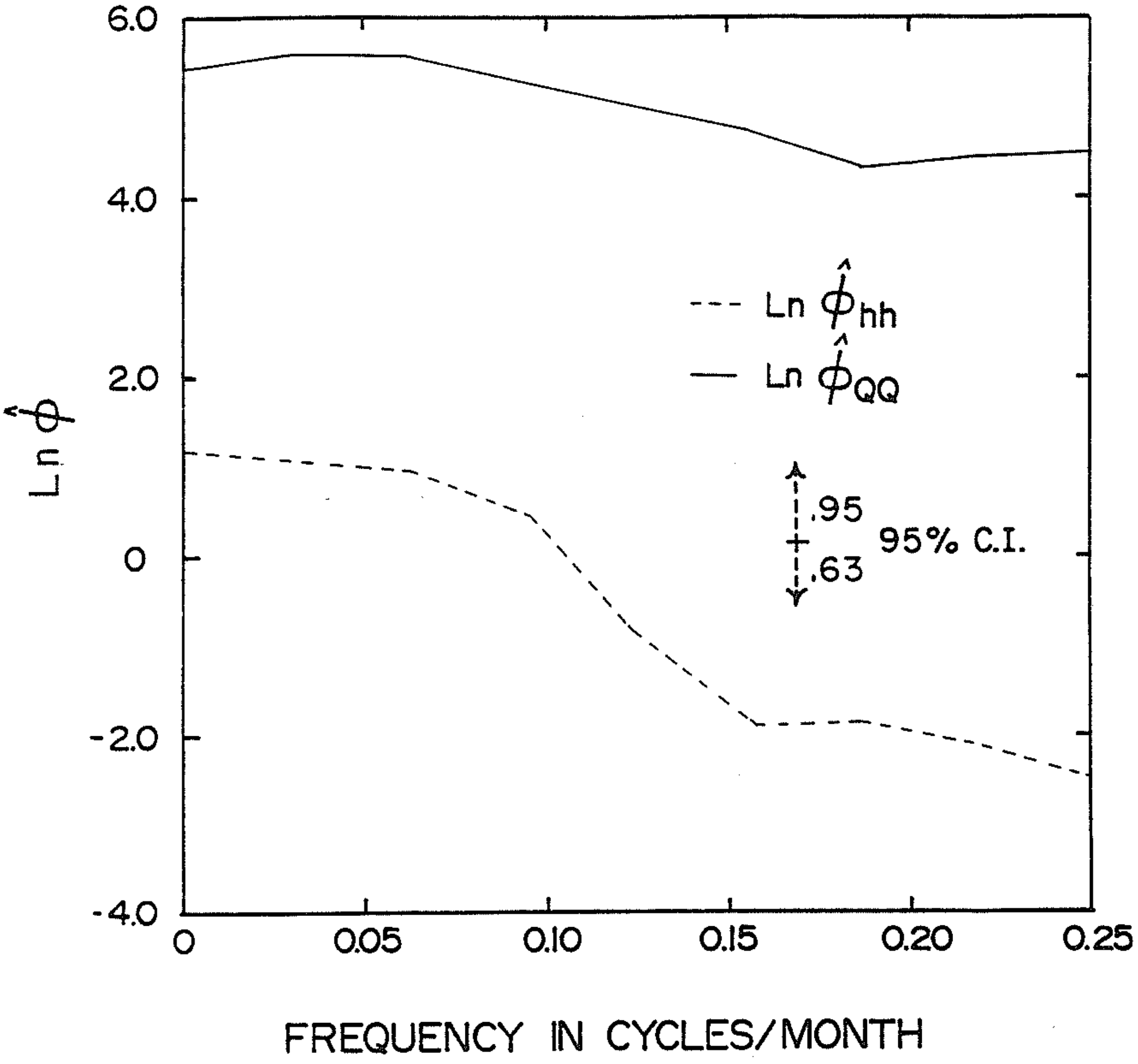

Fig. B.2: Spectral estimates of water level at Well No. 11 (Ln $\hat{\phi}_{hh}$) and discharge at Diamond 'A' Ranch (Ln $\hat{\phi}_{QQ}$), versus frequency. Data listed in Table B.III.

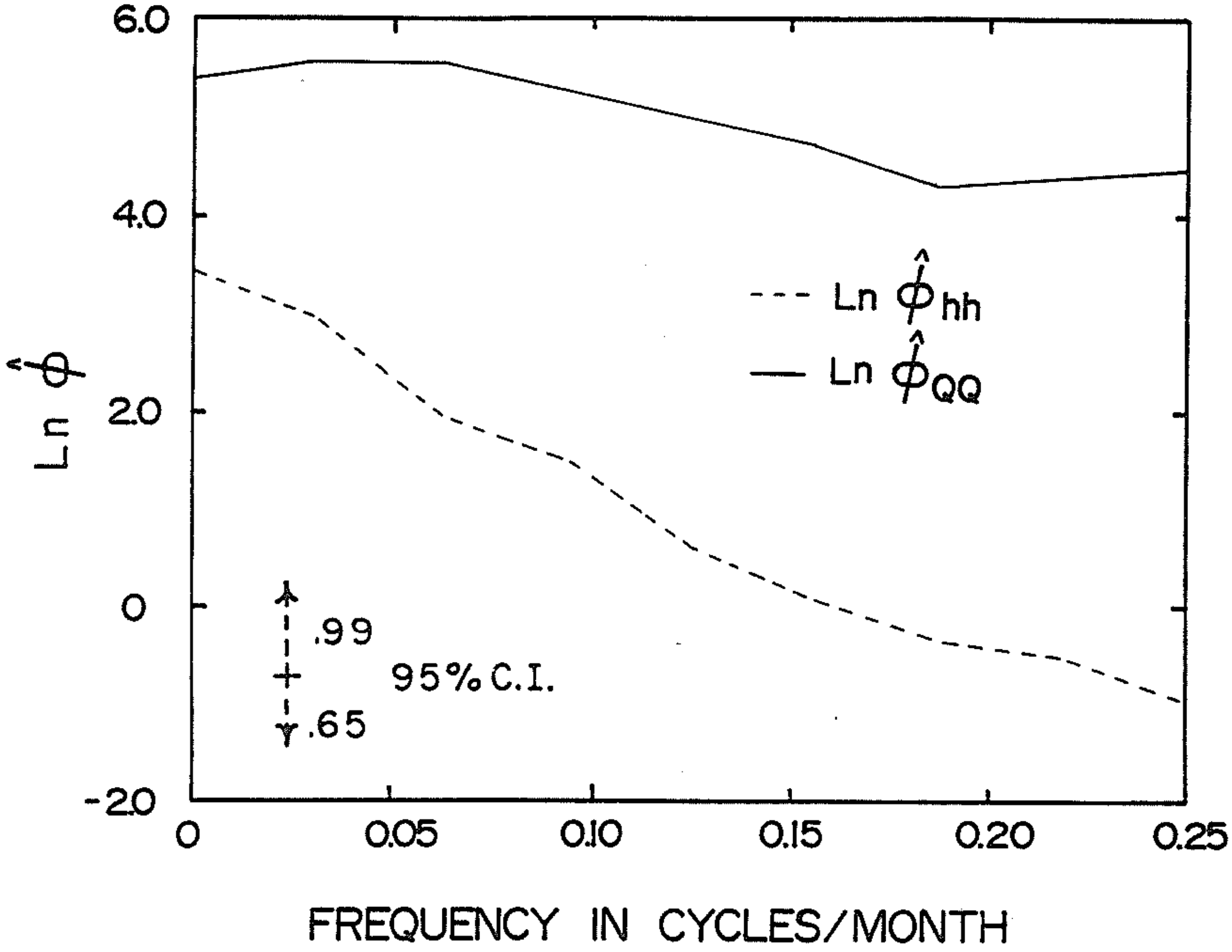

Figure B.3: Spectral estimates of water level at Well No. 12 ($\text{Ln}\,\hat{\phi}_{hh}$) and discharge at Diamond 'A' Ranch ($\text{Ln}\,\hat{\phi}_{QQ}$), versus frequency. Data listed in Table B.III.

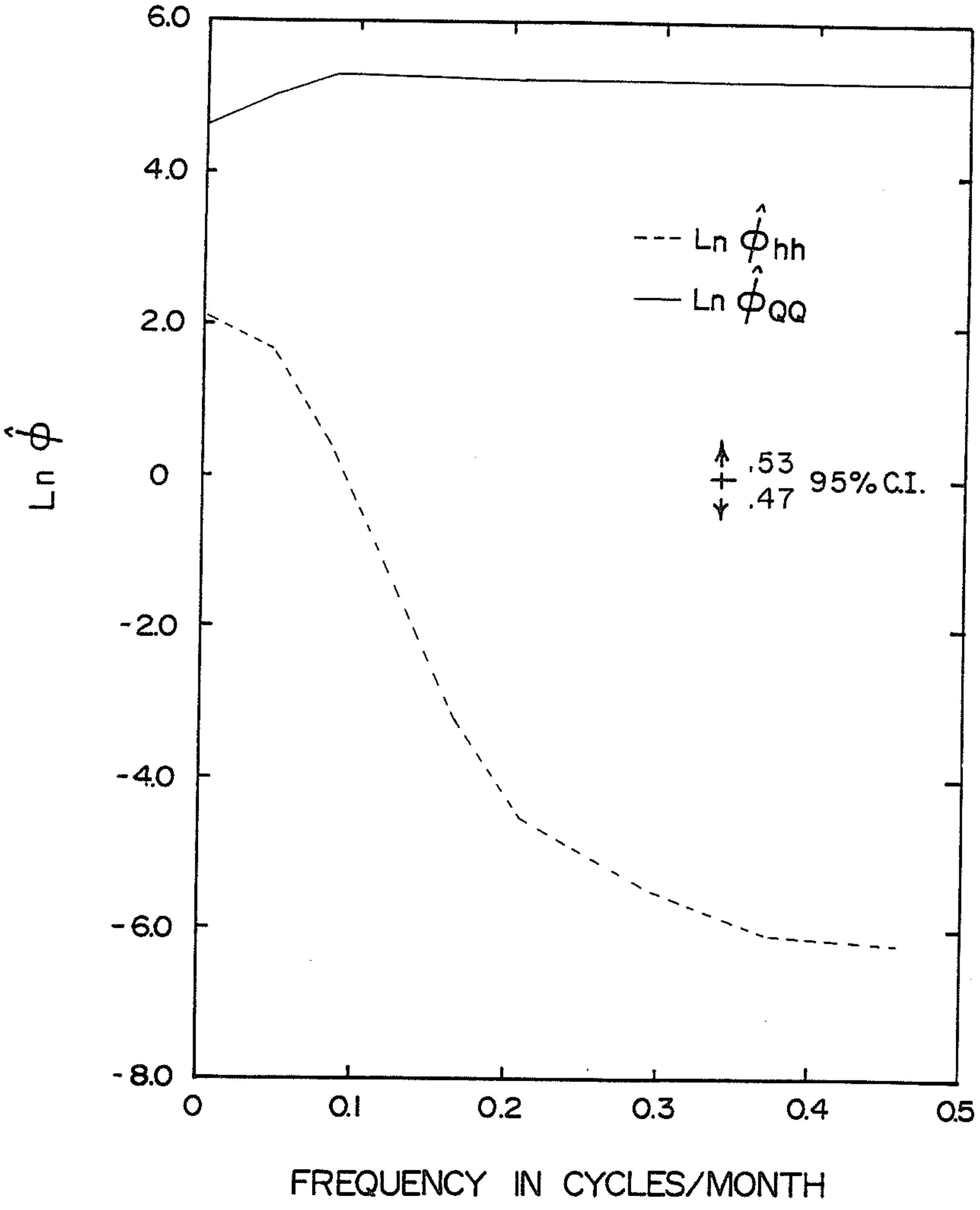

Fig. B.4: Spectral estimates of water level at Observation Well No. 7 (Ln $\hat{\phi}_{hh}$) and discharge at Dayton (Ln $\hat{\phi}_{QQ}$), versus frequency. Data listed in Table B.IV.

Table B.II. Listing of Spectral Estimates and Ln Spectral Estimates for Well No. 8 and Stream Discharge at Diamond 'A' Ranch.

Observation Well No. 8

Frequency (cycles/month)	Spectral Estimates ϕ_{hh}	$\text{Ln}\phi_{hh}$
0.0	21.11	3.05
0.025	21.30	3.06
0.050	13.15	2.58
0.075	3.90	1.36
0.100	1.48	.389
0.125	.824	- .194
0.150	.578	- .549
0.175	.460	- .777
0.200	.245	-1.409
0.225	.154	-1.868
0.250	.154	-1.868
0.275	.078	-2.55
0.300	.053	-2.94
0.325	.038	-3.28
0.350	.040	-3.21
0.375	.035	-3.34
0.400	.025	-3.68
0.425	.016	-4.17
0.450	.010	-4.61
0.475	.007	-4.94
0.500	.024	-3.75

Continued

Table B.II. Continued.

Discharge at Diamond 'A' Ranch

Frequency (cycles/month)	Spectral Estimates ϕ_{QQ}	$\mathrm{Ln}\phi_{QQ}$
0.0	206.35	5.33
0.025	273.71	5.61
0.050	303.68	5.72
0.075	287.62	5.66
0.100	238.32	5.47
0.125	205.29	5.32
0.150	180.11	5.19
0.175	104.91	4.65
0.200	52.60	3.96
0.225	70.57	4.26
0.250	96.82	4.57
0.275	125.14	4.83
0.300	106.94	4.67
0.325	69.32	4.24
0.350	103.71	4.64
0.375	110.62	4.71
0.400	76.14	4.33
0.425	68.46	4.22
0.450	65.56	4.18
0.475	61.06	4.11
0.500	61.95	4.13

Table B.III. Listing of Spectral Estimates and Ln Spectral Estimates for Wells No. 11, 12 and Stream Discharge at Diamond 'A' Ranch (9 Lags).

Well No. 11

Frequency (cycles/month)	Spectral Estimates ϕ_{hh}	 $\mathrm{Ln}\phi_{hh}$
0.0	3.29	1.189
0.031	2.77	1.020
0.063	2.46	.900
0.094	1.68	.521
0.125	.422	- .864
0.156	.163	-1.817
0.188	.163	-1.812
0.219	.1306	-2.035
0.250	.0839	-2.478

Well No. 12

Frequency (cycles/month)	Spectral Estimates ϕ_{hh}	 $\mathrm{Ln}\phi_{hh}$
0.0	31.470	3.448
0.031	19.48	2.969
0.063	7.253	1.980
0.094	4.915	1.592
0.125	1.946	.666
0.156	1.128	.120
0.188	.675	- .3937
0.219	.567	- .567
0.250	.399	- .9178

Continued

Table B.III. Continued.

Discharge at Diamond 'A' Ranch

Frequency (cycles/month)	Spectral Estimates	
	ϕ_{QQ}	$Ln\phi_{QQ}$
0.0	227.590	5.427
0.031	269.784	5.598
0.063	270.007	5.598
0.094	198.073	5.289
0.125	151.213	5.019
0.156	116.130	4.755
0.188	78.796	4.366
0.219	84.871	4.441
0.250	87.907	4.476

Table B.IV. Listing of Spectral Estimates and Ln Spectral Estimates for Well No. 7 and Stream Discharge at Dayton.

<u>Observation Well No. 7</u>

Frequency (cycles/month)	Spectral Estimates ϕ_{hh}	$Ln\phi_{hh}$
0.0	8.31	2.117
0.042	5.31	1.669
0.083	1.369	.313
0.125	.209	-1.566
0.167	.0404	-3.208
0.208	.0108	-4.525
0.250	- .0014*	
0.292	.0041	-5.476
0.333	- .0035*	
0.375	.00219	-6.122
0.417	- .0030*	
0.458	.0020	-6.19
0.500	- .0015*	

*Note: Negative spectral estimates are not used.

Continued

Table B.IV. Continued.

Discharge at Dayton

Frequency (cycles/month)	Spectral Estimates ϕ_{QQ}	$Ln\phi_{QQ}$
0.0	102.577	4.631
0.042	161.140	5.082
0.083	206.333	5.329
0.125	200.622	5.301
0.167	198.578	5.291
0.208	195.499	5.276
0.250	193.269	5.264
0.292	191.168	5.253
0.333	189.847	5.246
0.375	189.146	5.242
0.417	188.248	5.238
0.458	188.535	5.239
0.500	187.93	5.236